NASA

Technical Memorandum 86086

STREAM DYNAMICS BETWEEN 1 AU AND 2 AU: A DETAILED COMPARISON OF OBSERVATIONS AND THEORY

L. Burlaga
V. Pizzo
A. Lazarus
P. Gazis

APRIL 1984

National Aeronautics and
Space Administration

Goddard Space Flight Center
Greenbelt, Maryland 20771

STREAM DYNAMICS BETWEEN 1 AU AND 2 AU: A DETAILED COMPARISON OF OBSERVATIONS AND THEORY

L. F. Burlaga
NASA/Goddard Space Flight Center
Laboratory for Extraterrestrial Physics
Greenbelt, MD 20771

V. Pizzo
High Altitude Observatory
NCAR, P. O. Box 3000
Boulder, CO 80307

A. Lazarus
Center for Space Research
Massachusetts Institute of Technology
Cambridge, MA 02139

P. Gazis*
Center for Space Research
Massachusetts Institute of Technology
Cambridge, MA 02139

*Current Address: NASA/Ames Research Center, Moffett Field, CA 94035

ABSTRACT

A radial alignment study of three solar wind stream structures observed by IMP-7 and -8 (at 1.0 AU) and Voyager 1 and 2 (in the range 1.4 - 1.8 AU) in late 1977 is presented. It is demonstrated that several important aspects of the observed dynamical evolution can be both qualitatively and quantitatively described with a single-fluid 2-D MHD numerical model of quasi-steady corotating flow, including accurate prediction of: 1) the formation of a corotating shock pair at 1.75 AU in the case of a simple, quasi-steady stream; 2) the coalescence of the thermodynamic and magnetic structures associated with the compression regions of two neighboring, interacting, corotating streams; and 3) the dynamical "destruction" of a "small" (i.e., low velocity-amplitude, short spatial-scale) stream by its overtaking of a slower moving, high-density region associated with a preceding transient flow. The evolution of these flow systems is discussed in terms of the concepts of "filtering" and "entrainment", which have appeared in the literature. It is concluded that this study provides support at a detailed, quantitative level for our general conceptual notions of stream evolution in the inner solar system.

1. Introduction

The study of dynamics of interplanetary stream evolution has progressed to the point that it can by legitimately claimed that the basic processes are fairly well understood. It was early appreciated (Parker, 1963; Sarabhai, 1963) that large scale inhomogeneities in solar wind flow speed associated with the quasi-steady global structure of the corona would, under the influence of solar rotation, give rise to a spiral interaction front in interplanetary space. At the leading edge of the structure, kinematic steepening would occur as fast material overtakes slower material previously emitted from the corona, thereby compressing the gas caught between the two flows. Likewise, at the trailing edge of the high-speed stream, a rarefaction would form as fast material outruns the succeeding slow flow. If the speed differences in the two flows were great enough, forward and reverse shock waves could be expected to form at the edges of the compression region. Quantitative models (e.g., Hundhausen, 1973a) suggested shock pairs might form as near to the sun as 1 AU, and simple dynamical considerations dictated these structures should survive well out into the solar system (Hundhausen, 1973b). A reverse shock was observed at 1 AU by Burlaga, 1979, but in general, corotating shocks are rarely seen at 1 AU (Ogilvie, 1972). Observations by Pioneer 10 and 11 subsequently confirmed that shock pairs form between 1 AU and 4 or 5 AU (Hundhausen and Gosling, 1976; Smith and Wolfe, 1976, 1977; Dryer et al., 1978), where numerous sawtooth velocity structures were detected. These structures (dubbed corotating interaction regions or CIR's) represent the more advanced stages of stream evolution, in which the material entrapped at the stream front has achieved its maximum compression and is reexpanding, driving a forward-reverse shock pair back into the surrounding flow. It was found the entire process could be nicely modeled with a relatively simple nonlinear hydrodynamic formulation (Gosling et al., 1976), though some approximation to the field behavior would be obviously required to provide a more complete analysis (e.g., Dryer et al., 1978).

Though the gross aspects of stream evolution appear to have been satisfactorily explained, a great many details remain to be worked out. In recent years, for example, considerable attention has been devoted to the quantitative evaluation of the dynamic mechanisms by which the gas at the

leading edge of a high-speed stream responds to the kinematic steepening imposed by the velocity structure (Goldstei', 1971; Pizzo, 1980, 1981, 1982; Whang and Chien, 1981). Gas and magnetic pressure gradients built up in the compression region give rise to nonradial flows, which leads to lateral slippage between the colliding fast and slow streams. The net effect is that the dynamic reaction of the gas tends to oppose the kinematic steepening, resulting in a less severe, spatially broadened compression and a correspondingly reduced rate of shock formation. These effects are thought to be particularly important out to about 1 AU and at least partially explain some of the not insubstantial discrepancies between theory and observation in that region. (See Pizzo, 1983, for a more complete discussion of this problem.)

In view of the wealth of data and more sophisticated models currently available, it would be instructive to combine the two in taking a harder and more detailed look at the various dynamical processes occurring in the interplanetary solar wind. To this end, we have assembled a set of plasma and field data from 1977, when Voyager 1 and 2 were situated between 1.4 and 1.8 AU and were favorably radially aligned with the earth-orbiting IMP-7 and -8 spacecraft as well as with each other. Three successive stream structures from this period will be analyzed with the help of a single fluid, 2-D MHD corotating flow model to illustrate several interesting features of the evolution and to provide a theoretical basis for their interpretation.

The first structure to be discussed is the simplest one, appearing at 1 AU as a classic steepened (but not shocked) quasi-steady high speed stream. It is demonstrated that the model successfully predicts the formation of a forward-reverse shock pair that was subsequently observed by Voyager 1 at 1.74 AU and also reproduces the observed plasma and magnetic variations with reasonable accuracy.

The second case involves a more complicated situation, in which one fast corotating stream overtakes a slower, preceding corotating stream. While the same physics operative in the simple stream still applies, it should come as no surprise that certain details of the process will differ. Here both the faster and slower streams are individually evolving at somewhat different

rates, while at the same time the faster, "bigger" one advances upon (and sweeps up) the slower, "smaller" one. We shall be paying particular attention to the thermodynamic and magnetic structures of the two streams, for as the evolution proceeds the compression regions of the individual streams are eventually advected together, resulting in a single, merged compression at the front of a single, merged stream. Again, the model is shown to describe the observed processes quite well.

In the third case, we consider what happens when a "small" corotating stream overtakes a transient high density region behind a shock. Comparison of the observations with the model demonstrates that the stream is effectively destroyed in the interaction, i.e., that all the high speed material in the stream is consumed by the dynamic exchange of momentum with the dense material of the transient flow.

Together, these studies bolster our confidence in the ability of 2-dimensional MHD models to replicate the dynamic behavior of the solar wind near and beyond 1 AU and lend further credence to our general conceptual picture of stream evolution. Moreover, they also serve as excellent illustrations of the dynamical processes that have been variously described in the literature as either "filtering" (Gosling et al., 1976) or "entrainment" (Burlage et al., 1983a) and will therefore be used as a springboard to a discussion of this subject in the final passages of this paper.

2. Overview of the Flows, Spacecraft Trajectories and Data Sets

For the purposes of this study, we shall make use of the solar wind flows observed by IMP 7 and 8 at 1 AU and Voyager 1 and 2 at 1.4-1.7 AU in the time period between ∿ November 10 and ∿ December 25, 1977. The speed profile observed by IMP-7 and -8 at 1 AU in this period is plotted in Figure 1 together with a map of coronal holes from the HAO. The coronal hole map has been shifted in time corresponding to the transit time to 1 AU, so that the streams and the corresponding coronal holes are nearly vertically aligned. Three flows predominate in the interval. The first and third flows (labeled 1 and 3 in Figure 1) apparently originated in an equatorial extension of a lobe of the north polar coronal hole, and they represent a recurrent and hence a "corotating flow". Note, however, that neither the streams nor the coronal holes are unchanged from one rotation to the next), through they are steady enough to be classified as corotating flows, on the basis of solar wind data. Such flows were discussed by Burlaga et al. (1978) and Rhodes and Smith (1981). Stream 2 is associated with a lobe of the south polar coronal hole, and it has negative polarity for the most part.

Closer inspection of the magnetic field and speed profiles of streams 1 and 2 suggests that they are actually "compound streams" (Burlaga and Ogilvie, 1970), each consisting of two separate streams. The initial part of stream 1 has "anomalous" negative polarity, whereas the body of the stream has positive polarity consistent with its source being a positive polarity, northern hemisphere coronal hole. Similarly, the initial part of stream 2 has mixed polarity, whereas the region with highest speeds has negative polarity consistent with its source being a southern hemisphere coronal hole. (Cross-hatched regions in Figure 1 indicate missing magnetic field data.) Stream 3 is relatively uncomplicated, with uniform positive polarity, and it can be thought of as a simple corotating stream.

The trajectories of Voyagers 1 and 2 (hereafter abbreviated V1 and V2, respectively) and of IMPs 7 and 8 are shown in inertial heliographic (IHG) coordinates in Figure 2. X_{IHG} and Y_{IHG} are the coordinate axes in the solar equatorial plane: X_{IHG} points along the longitude of the ascending node. The latitude angle λ between the Sun-spacecraft line and the solar equatorial

plane is plotted versus X_{IHG} in Figure 2. Owing to the tilt of the sun's equatorial plane relative to the ecliptic, the heliographic latitude of Earth (hence also IMP-7 and IMP-8) oscillates between +7.5° and -7.5° in the course of the year. V1 was very close in latitude to IMP-7 and IMP-8 throughout most of the interval of interest, while V2 was at somewhat higher latitudes. IMP-7 and IMP-8 were radially aligned with V1 and V2 near November 20, and the alignment was close to radial throughout the time interval, the misalignment being greatest for stream 3. Since the IMP-V1 alignment was generally better and since there are only minor differences between the V1 and V2 observations, for clarity only the V1 data will be used in the plots.

This study was based primarily upon hourly averages of the magnetic field strength and components from the GSFC magnetometers on IMP-8, V1 and V2, and hourly averages of the proton density, temperature and bulk velocity from the MIT plasma experiments on IMP-7, IMP-8, V1 and V2; some higher resolution data will be discussed in relation to the identificataion of shocks and discontinuities. Owing to instrumental problems, magnetic field data and measurements of density and temperature are not available from IMP-7, so there are gaps of ~4 days in those parameters every ~8 days (when IMP-8 was in the magnetosphere). Thus, our 1 AU baseline data consist of nearly continuous measurements of the bulk speed from IMPs-7 and -8, and measurements of the magnetic field, density, and proton temperature from IMP-8 alone. There are also small gaps of less than a few hours duration every day or so, but these can reasonably be filled by linear extrapolation, since the stream profiles generally change very little on a scale of a few hours. These data are from the compilation of King (1979). The Voyager data set is more nearly complete, with measurements available nearly every day, but there are intermittent tracking gaps of several hours duration. Again these can generally be filled by extrapolation.

3. The Model and Its Application to the Data

An essential part of the analysis is to feed data from one spacecraft at lesser heliocentric distance into a dynamical model and map the evolution to a suitably aligned spacecraft at a greater heliocentric distance, and to compare the theoretical predictions with the second set of observations. Burlaga and

Ogilvie (1970) showed that the magnetic pressure is comparable to the thermal pressure in interaction regions at 1 AU, and they stressed that a magnetohydrodynamic theory is needed to describe their behavior. MHD models of flows beyond 1 AU have been presented by Dryer et al. (1976, 1978), Goldstein and Jokipii (1977), and Pizzo (1983). The numerical model employed here is a planar version of the single-fluid 3-D formulation of Pizzo (1982). Since the model is described in great detail in the work cited, only a brief outline is presented here.

The 2-D nonlinear, polytropic MHD equations are used to describe large-scale, quasi-steady, corotating flow dynamics in interplanetary space. In an inertial (non-rotating) frame, the single-fluid equations in conservation form are:

(mass)

$$\frac{\partial}{\partial r}(r^2 \rho u_r) = -r \frac{\partial}{\partial \phi}(\rho v_\phi) \tag{1}$$

(radial momentum)

$$\frac{\partial}{\partial r}\left[r^2 \left(\rho u_r^2 + P - \frac{B_r^2 - B_\phi^2}{8\pi}\right)\right] = \tag{2}$$

$$- r \frac{\partial}{\partial \phi}\left(\rho u_r v_\phi - \frac{B_r B_\phi}{4\pi}\right) + r\left[\rho\left(u_\phi^2 - \frac{GM}{r}\right) + 2P + \frac{B_r^2}{4\pi}\right]$$

(azimuthal momentum)

$$\frac{\partial}{\partial r}\left(r^3 \left(\rho u_r u_\phi - \frac{B_r B_\phi}{4\pi}\right)\right) = \tag{3}$$

$$- r^2 \frac{\partial}{\partial \phi}\left(\rho u_r v_\phi + P + \frac{B_r^2 - B_\phi^2}{8\pi}\right)$$

(Maxwell's equation)

$$\frac{\partial}{\partial r}(r^2 B_r) = -r\frac{\partial}{\partial \phi} B_\phi \tag{4}$$

(total energy)

$$\frac{\partial}{\partial r}\left(r^2\left(u_r\left(\frac{\rho u^2}{2} + \frac{\gamma}{\gamma - 1}P\right) - \frac{wB_r B_\phi}{4\pi}\right)\right) = \tag{5}$$

$$-r\frac{\partial}{\partial \phi}\left(v_\phi\left(\frac{\rho u^2}{2} + \frac{\gamma}{\gamma - 1}P\right) + w\left(\frac{(B_r^2 - B_\phi^2)}{8\pi} + P\right)\right) - \rho u_r GM$$

where

$$u^2 = u_r^2 + u_\phi^2,$$

$$w = \Omega r,$$

and

$$v_\phi = u_\phi - \Omega r,$$

where v_ϕ is the azimuthal velocity in the rotating frame.

The two independent variables are the spherical components (r,ϕ), and the five dependent variables are the radial and azimuthal velocity components u_r and u_ϕ, the radial magnetic field B_r, and the two thermodynamic variables, density ρ and gas pressure P. Pressure is defined by the perfect gas law as

$$P = 2nkT, \tag{6}$$

where n is the proton number density ($= \rho/m_p$), k is Boltzmann's constant, and T is the single-fluid temperature. For purposes of computation, T at 1 AU is obtained by taking the average of the observed proton temperature T_p and a presumed constant electron temperature $T_e = 1.25 \times 10^{4o}$K.

Since the field is effectively tied to the flow in the rotating frame due the high electrical conductivity of the medium, the azimuthal component of the field is given by

$$B_\phi = \frac{v_\phi}{u_r} B_r \qquad (7)$$

In the 2-D approximation, only flow within the equatorial plane is considered, so $u_\theta = B_\theta = \partial/\partial\theta = 0$, where θ is the meridional (north-south) coordinate in the spherical system. Thus all structures are assumed to be uniform along meridional arcs and are oriented perpendicular to the equatorial plane. Finally, the internal energy is dictated by a polytrope law [incorporated in the total energy equation (5)]. The polytropic index, γ, for the single fluid gas is assigned the value 5/3; the results are not sensitive to the choice of γ. Two fluid models were also examined, but there was little difference between the predictions of this model and those of the 1-fluid model (see the Summary and Discussion). The remaining physical constants in (1)-(5) are Ω, the mean solar rotation rate; G, the universal gravitational constant; and M, the solar mass.

The numerical integration of the equations is fully discussed in Pizzo (1982) and only a brief synopsis is needed here. Values for the dependent variables are specified at each discrete ϕ at some initial r and are propagated to $r + \Delta r$ by means of the two-step explicit scheme of MacCormack (1971). The radial step size Δr is determined from the Courant condition, taking into account additional constraints imposed by the small amounts of artificial viscosity introduced to maintain computational stability in the presence of corotating shocks and discontinuities.

The incorporation of real data into the model requires a string of input data evenly spaced in azimuth (longitude), all gathered at a single, fixed heliocentric distance r. Hourly averages from the Earth-orbiting IMP spacecraft fit this prescription quite closely, requiring only a simple conversion from time to longitude. For the large-scale structures to be modeled here, the resulting $\Delta\phi$ resolution of about 0.5° is quite adequate to follow the evolution. Hourly averages from the more distant Voyager

spacecraft provide the same azimuthal resolution, but an added complication arises from the radial motion of the spacecraft. The Voyagers typically travel one-tenth AU in heliocentric distance during the time it takes for the complete stream structure to pass by. For exactitude in the model-data comparison, we should either interpolate the model output to the instantaneous position of Voyager or, less palatably, correct the data to some common r by arbitary means. For the level of accuracy required in this study, though, we have elected to simply overlay on the raw Voyager time sequence the output of the model at a fixed r chosen such that the Voyager and model radii coincide in the middle of the interaction region. In this way, the largest radial position displacement between the two curves is limited to about .01 AU in the vicinity of the dynamic structures of greatest interest. The point where the data and model coordinates exactly coincide is indicated in the plots by the triangle along the bottom.

Data gaps in the input have been filled by linear interpolation. Where only a few hours data are missing, little degradation in the mapping is experienced. However, where the gaps are more serious, particularly in the IMP record, spurious behavior is evident in the theoretical predictions. Fortunately, since the flow is highly supersonic and the radial span of the mapping is fairly small, these artifacts are relatively localized and the tainted portions of the solution can be readily identified and discarded. Similarly, the treatment of the longitudinal ends of the data string, which are arbitrarily forced to be periodic for computational considerations, has has negligible influence on the main part of the solution.

In specifying the magnetic field input, we are presented with a choice, since the spacecraft data contain more information that is compatible with the corotating formulation. That is, once u_r and u_ϕ are set, then the field-aligned condition (7) dictates that only one element of information about the field can be entered into the initial conditions. We could specify B_r or B_ϕ directly from the data, but the behavior of the components of $\vec{B}$ in the solar wind is generally dominated by waves and small-scale transient structures. This problem becomes especially acute at large heliocentric distances, where hourly averages of the components are not representative of the mean field and determination of the field magnitude at the lowest levels

might be subject to uncertainty. On the other hand, it is $|\vec{B}|$ which is the important physical parameter, for the main large-scale magnetic driving force in interplanetary space is the magnetic pressure force, not tension. Furthermore, $|\vec{B}|$ regulates the characteristic speed at which small-amplitude disturbances propagate and are a prime factor in the relaxation of CIR's. In the model calculations, B_r on the initial surface is fixed by the relation

$$B_r = \frac{|\vec{B}|}{\left(1 + \frac{v_\phi^2}{u_r^2}\right)^{1/2}},$$

where $|\vec{B}|$, v_ϕ, and u_r are the observed quantities. Since all magnetic force terms in the corotating formulation are independent of the polarity of B_r, the positive sign is always chosen. Magnetic sectors may be passively mapped by following the motion of select tracer particles in the flow and reversing the polarity across the appropriate boundaries after the fact. Of course, the dynamics associated with the current sheet transition are not accounted for, but these effects should be quite localized and negligible on the large scale.

4. Classic Corotating Stream

We first consider the radial evolution of the simple corotating stream labeled "stream 3" in Figure 1. Five-minute averages of the basic parameters measured at 1 AU (Figure 3) show a stream interface and an interaction region ahead of a fast stream, but there is no indication of a forward or reverse shock. Hourly averages of these data, shown on the left of Figure 4, were used as inputs to the MHD model, and the predicted profiles at 2 AU are shown at the right of Figure 4. Note that the interface survives to 2 AU, and more importantly a forward and reverse shock pair are present at 2 AU, forming the boundaries of a relatively simple pressure wave. Voyager 1 observed this stream at 1.74 AU, and the observations as well as the MHD model predictions at this distance are shown in Figure 5. This figure shows that a corotating forward and reverse shock pair are both predicted and observed. The predicted shocks arrive slightly earlier than the observed shocks (an error of $< 5^{\circ}$ in Carrington longitude or $\lesssim$ 10% error in the propagation time between 1 AU and 1.74 AU). This small difference can be attributed to variations associated with the departures from radial alignment and possibly temporal and latitudinal variations.

The existence of the forward-reverse shock pair at 1.74 AU is shown more clearly in Figure 6 which gives a plot of 9.6s averages of the magnetic field and measurements of the plasma parameters. The forward shock is very thin, the transition occurring in < 9.6 sec. The reverse shock is somewhat broader, with the density and thermal speed decreasing over an interval of several minutes, but it is still appropriate to regard it as a shock.

Returning to Figure 5, it is useful to compare the predicted and observed variations of some other flow parameters, the density, field strength, temperature, and total pressure. The longitudinal shift of the major features near the stream front is readily apparent, but the shapes of the profiles and their approximate amplitudes match reasonably well. A stream interface (marked I in the plot) is both predicted and observed, though shifted longitudinally by the same amount as the shocks. The two worst discrepancies involve the general underestimate of the temperature and the behavior of some of the other parameters, especially the density, following the reverse shock.

The former problem can be attributed to the single-fluid nature of the model (the T comparison is the one thing that can be significantly improved by recourse to the two-fluid formulation mentioned above), while the latter has its origins in the extended gap in the 1 AU data visible in Figure 4, left.

In summary, then, the observed speed profile is accurately reproduced by the model, there is generally good agreement in the density and field strength profiles, and the temperature and pressure profiles show the same qualitative features. The relative positions of the forward fast shock and the stream interfaces are also accurately determined by the model. This is particularly significant because the shocks are handled by introducing a finite artificial viscosity to cope with rapid variations in plasma parameters. We conclude that the model is reliable over the distances considered and therefore feel justified in its further application in this paper.

Finally, to illustrate how this stream relates to our preconceptions of CIR formation, Figure 7 presents a projection of the flow out to 4 AU. There the stream appears as the typical saw-tooth velocity structure, with forward and reverse shocks bounding and expanding compression region. The high speed material in the stream is being eroded by the reverse shock while the slow flow ahead of the CIR is being accelerated by the forward shock. The CIR continues to broaden with distance until eventually it begins to interact with neighboring CIR's (see also Burlaga, 1983; Pizzo, 1983).

5. Interaction of Adjacent Slow and Fast Corotating Streams

In the interval November 10-16, 1977, IMP-8 at 1 AU observed one corotating stream flow immediately followed by a faster corotating stream, as shown in a plot of 5 min averages in Figure 8. This compound stream is labeled "stream 1" in Figure 1. A stream interface was observed late on November 10, across which the density dropped while both the temperature and the bulk speed increased. As the speed continued to increase during the day following the interface, we may describe this structure as a slow corotating stream. There is some evidence for the formation of a forward shock on November 10 and possibly a reverse shock on November 11, which might be part of the same flow pattern. A relatively large and fast corotating stream was observed on November 14 and 15, presumably originating in the trans-equatorial coronal hole shown in Figure 1. The magnetic field polarity of this stream differs from that of the preceding stream indicating that they had different sources. A diffuse interface between the two flows was observed on November 14, though no forward or reverse shocks were seen by IMP-8. Because the corotating stream on November 14 and 15 was moving faster than that of the November 11 flow, one expects it to overtake, collide with and "sweep-up" the latter. The nature of that interaction is the principal topic of this Section.

Figure 9 shows a plot of the connected hourly averages of B, V, N, T and P_T (the magnetic plus proton pressure) versus relative heliocentric azimuth. The IMP-8 profiles on the left of Figure 9 were used as inputs to the MHD model, and the computed profiles at 2 AU are shown on the right of Figure 9. At 1 AU (Figure 9, left), both the magnetic field and the pressure show two maxima, one at each of the interfaces. Thus there are two compressions, one associated with the interaction region of the slow corotating flow, and the other associated with the interaction region of the fast corotating flow. The magnetic field profile is very similar to the total pressure profile, indicating the importance of the magnetic pressure in the dynamics. At 2 AU (Figure 9, right), in contrast to the two broadly spaced peaks in the pressure profile at 1 AU, there is a single peak. The same pattern is seen in the magnetic field profile: a single maximum in B is predicted at 2 AU whereas two widely-spaced maxima were observed at 1 AU. Thus, the model predicts a qualitative change in the total pressure and magnetic field profiles between 1 AU and 2 AU.

The qualitative change just described occurs because the advection of the fast corotating stream relative to the slower flow brings their separate compression regions (also referred to in the literature as corotating pressure waves; Burlaga et al., 1983) closer together while at the same time each compression region wave is expanding. The amplitude of the stream at 2 AU (see Figure 9) is diminished because some of the kinetic energy of the high-speed material from the streams is continually being fed into the growth of their respective compression regions between 1 AU and 2 AU. The mechanism for this increase is kinematic steepening (e.g., see Hundhausen, 1972, Burlaga and Barouch, 1976; and Gosling, 1981). Thus the amplitude of the corotating pressure wave ahead of the fast stream grows relative to that ahead of the slower stream. At the same time, the expansion of the two compression regions tends to fill in and close the region of low pressure seen at 1 AU, so that by 2 AU there is a single compression which is formed by the coalescence of two separate corotating pressure waves.

The above scenario is qualitative and intuitive, of course, and while the validity of the model in the case of the simple corotating stream has been confirmed, it has not been unequivocally demonstrated under these circumstances. More quantitative results and additional insight can therefore be obtained by comparison of the predictions of the model with observations. In this case, we compare predictions of the model with data from Voyager 1 that were obtained near 1.44 AU. The results are shown in Figure 10 with the predictions of the model shown by the solid curves and the Voyager observations shown by dots.

Figure 10 shows that at 1.44 AU there were two broad humps in the pressure profile instead of the two narrower peaks seen at 1 AU. The model predicts the development of a reverse shock associated with the slow stream. This is the feature that was identified as a potential reverse shock on November 11 in Figure 8. A fully developed reverse shock was not seen by Voyager 1 but the observed general variation of the flow parameters near the predicted shock position did resemble the calculated pattern (see Figure 10). Thus, we may say at least that the interaction region ahead of the slow stream was probably expanding backward toward the sun at a speed comparable to the

magnetoacoustic speed, further broadening the interaction region, reducing the amplitude of the compression region, decelerating the stream, and filling the low pressure region observed at 1 AU. Of course, these features could not be derived from a kinematic model; dynamical effects are fundamental in the evolution of interaction regions.

The interaction region associated with the fast corotating stream in Figure 10 shows a peak in P_T near the interface, but the pressure wave is rather broad and flat-topped. Neither a corotating forward shock nor a reverse shock is observed or predicted, but one can see a region (marked (RS) in Figure 10) where a reverse shock might be forming. The forward part of the corotating pressure wave ahead of the fast stream is just approaching the reverse part of the pressure wave associated with the slow stream (which has the signature of a reverse shock in the theoretical curves in Figure 10). Thus, the low pressure region between the two pressure waves is narrow at 1.44 AU and apparently being filled in rapidly. The agreement between predictions and observations in Figure 10 gives us further confidence in the accuracy of the model. In particular, the coalescence of the compression regions (pressure waves) predicted to occur between 1 AU and 2 AU must be taken seriously, as the Voyager observations at 1.44 AU are coveniently located to reveal the process in mid-stride. We can now proceed to describe some of the other features predicted by the model (Figure 9).

Two reverse shocks, at 2 AU, on the sunward side of the interface, are predicted by the model. One of the reverse shocks is a corotating reverse shock associated with the fast stream while the other is the corotating reverse shock associated with the slow stream. The reverse shock associated with the slow stream moved through the interface associated with the fast stream before it reached 2 AU. This caused an additional compression of the corotating interaction region ahead of the fast stream, giving a further enhanced pressure at its interface. Of course, the low pressure region seen between the two pressure waves was also compressed by this reverse shock as it moved through the slow stream toward and past the interface of the fast stream. Thus, the observation of 2 reverse shocks may be a signature of the interaction between 2 corotating streams. The coalescence of the two pressure waves seen at 1 AU into a single pressure wave at 2 AU is seen as the result

of several processes: 1) the slow stream pressure wave expands and drops in amplitude; 2) the fast stream pressure wave is advected forwarded, but does not diminish, since it is still being driven by the fast material; 3) where they meet there is further compression.

The model also suggests that other interesting interactions take place farther out, producing by 4 AU a single CIR with complex substructure. Figure 11 shows the speed profiles and the magnetic profiles (which are similar to the pressure profiles, not shown) predicted at 1 AU, 2 AU, 3 AU, and 4 AU. The most significant qualitative change between 2 AU and 4 AU is the coalescence of the two reverse shocks near 3 AU. This occurs because the reverse shock associated with the slow stream was moving faster than the reverse shock associated with the fast stream. It also appears that a forward shock associated with the fast stream forms near 2 AU and overtakes the forward shock associated with the slow stream just beyond 4 AU.

6. Destruction of a Corotating Stream overtaking a Transient Flow

We shall now describe the overtaking of a slow transient flow by a faster corotating stream. Coalescence of the two interaction regions is again observed, and in addition the destruction of the corotating stream is observed. This event has been discussed by Burlaga et al. (1980), who described the evolution of the corotating stream and suggested that the disappearance of the corotating stream between 1 AU and 1.6 AU was a dynamical effect. We shall give further details of the observations and show that the MHD model supports the conjecture that the corotating stream was destroyed by a dynamical interaction.

The IMP-8 observations at 1 AU are shown in Figure 12 for the period November 25 to December 1, 1977. Three flow configurations can be seen: 1) a transient flow on November 25, consisting of a forward shock (F1), followed by a shell of very high density material (> 100 cm^{-3}), followed in turn by a region of strong magnetic fields moving relatively slowly; 2) a corotating stream with a well-defined stream interface (IF) on November 26, and 3) a shock (F3) on November 29. The shock F3 apparently did not interact with the other flows inside of 2 AU, so we shall first consider the interaction of the corotating stream with the transient flow ahead of it.

Figure 13 shows the connected hour-averages of B, V, N, T, and P_T measured at 1 AU together with the corresponding profiles at 2 AU computed from the MHD model. Ignoring for the moment the transient flow corresponding to F3, one sees two compression regions near 270° at 1 AU, but only one broad compression region at 2 AU. The two pressure waves at 1 AU correspond to the interaction regions of the transient flow and the corotating flow, respectively.

The predictions of the model are compared with observations made at 1.6 AU by Voyager 1 in Figure 14. We see fairly good agreement between the theoretical speed profile and the observations, to within 20 km/sec over most of the time interval, and the basic qualitative features of N and B profiles are all reproduced by the model, with respectable quantitative agreement at higher values of N and B. The theoretical temperature and pressure profiles agree qualitatively with the observed profiles; there are some large

differences at times, which might be attributed to inhomogeneities of the flow, temporal effects, and to our neglect of electron measurements, but these are differences in detail. The position of the forward transient shock (F1) is accurately predicted. The model also predicts a corotating forward shock (F2) and a corotating reverse shock (RS). The corotating forward shock arrives slightly later than predicted, but this is again a detail which we shall not pursue in this paper. The model does accurately predict the time of arrival of the reverse shock. Detailed observations of the shocks themselves have been presented by Burlaga et al. (1980).

Figure 13 shows a narrow corotating stream with a maximum speed of $\sim$ 525 km/s associated with the interface at 1 AU, but at 2 AU the speed does not exceed 400 km/s; it is this change that we referred to above in speaking of the destruction of the stream. Since the 2 AU curves are theoretical profiles based on an MHD model of corotating streams, we have demonstrated that the destruction of a small corotating stream within 1 AU is theoretically possible for the input conditions given in Figures 12 and 13. (It should be emphasized that this case may not be typical, for the stream was relatively small and it collided with a region of unusually high density ($n > 100/cm^3$) associated with the transient shock.) It is firmly established, of course, that streams are destroyed (in the sense that velocity differences are wiped out by dynamic interaction) over spatial scales of several AU (Hundhausen and Gosling, 1976; Collard et al., 1982).

The two large pressure waves observed at 1 AU (see Figure 13 near 270°) are also seen at 1.6 AU (see the bottom of Figure 14). At 1.6 AU the corotating pressure wave was broader and had a higher amplitude than the transient pressure wave. It appears that these two waves were interacting and beginning to coalesce at 1.6 AU. The single broad pressure wave predicted at 2 AU (see Figure 13) is a natural extrapolation of the result seen in Figure 14. The corotating interaction region and the transient interaction region coalesce and become nearly indistinguishable by 2 AU, the result being a single merged interaction region.

Let us now consider the evolution of these flows to 3 AU. Figure 15 shows the speed and magnetic field strength profiles computed with the MHD

model, using as input conditions the IMP-8 data shown in Figure 13. One sees that the corotating forward shock F2 overtakes and interacts with the transient shock F1 at ~4 AU. The corotating reverse shock RS and the transient shock F3 interact somewhere between 2 AU and 3 AU. At 3 AU one sees a single broad interaction region in the B profile (the corresponding pressure profiles are not shown but they are qualitatively the same as the B profiles). This "interaction region" actually represents the coalescence of 3 separate interaction regions--those associated with the transient shock F1, the corotating stream, and the transient shock F3. Thus, we have at 3 AU a single merged interaction region and this is not associated with a fast stream!

7. Summary

We have discussed multispacecraft observations and an MHD model of the radial evolution of three flows between 1 AU and 1.74 AU using data from Voyager 1, IMP-7 and IMP-8. The first flow system (stream 3) was a simple, classic corotating stream. A forward-reverse shock pair was observed relatively close to 1 AU (v.z. 1.74 AU), and its development was predicted by the model. There was a small error in the predicted position of the shocks, which might be due to the small latitudinal separation of the spacecraft and/or to a temporal variation in the stream as it rotated through the several degree angle corresponding to the azimuthal separation of the two spacecraft. The second flow system consisted of a fast corotating stream overtaking a slower corotating stream. Two compression regioins (pressure waves) were observed at 1 AU, and these were computed to coalesce into a single pressure wave at 2 AU. The process was observed at mid-point by Voyager 1, confirming the gross predictions of the model. The third flow system consisted of a corotating stream overtaking a transient shock and flow. Again we observed two pressure waves at 1 AU which coalesced to form a single pressure wave at 2 AU. A third pressure wave associated with another transient shock at 1 AU was predicted to coalesce with the pressure waves just described, forming a single pressure wave at 3 AU from the 3 distinct pressure waves observed at 1 AU. This event was particularly notable because the corotating stream was effectively destroyed by its interaction with the transient flow inside of $\sim$ 1.6 AU.

The flows just described were modeled very satisfactorily with a stationary, 2-D, single-fluid MHD model. Comparison of predicted and observed flow features in all three cases demonstrates the general quantitative as well as qualitative validity of such models, down even to such details as shock formation and inspire some confidence in their predictions of dynamical behavior outside the realm of observation. The applicability of the 2-D assumption was discussed by Pizzo (1983); the justification for the 1-fluid formulation was investigated by comparing the results of this model with those computed for a 2-fluid model based on separate polytropic relations for protons and electrons. This latter model is essentially identical to that described by Goldstein and Jokipii (1977), the main difference being that

electron polytrope constant is chosen to be $\gamma_e = 1.175$. [See Scudder and Olbert (1979a,b) and Sittler and Scudder, 1980 for the theoretical and observational bases for using a polytrope description for solar wind electrons.] The differences in the V-T-N profiles for the two cases were negligible and the differences in the proton temperature profiles were small. Basically, this is because the contribution that the electrons make to the pressure is smaller than that due to the sum of the magnetic field pressure and the proton pressure, and hence the electron correction is negligible. The assumption of stationarity is valid for corotating structures like stream 1 and stream 3, but it is not obvious that it is appropriate for cases like stream 2, which involves a transient as well as a corotating flow. In fact, the model could not be applied if the spacecraft were not radially aligned. If the azimuthal separation were suitably large the transient flow might not even be seen by both spacecraft! However, we have analyzed a situation in which the spacecraft were nearly radially aligned, and we considered the evolution over relatively small distances. Under these circumstances, details of the azimuthal variations of the transient flow are not important to first approximation, since the effects of radial gradients are included in the stationary model. Thus, the good agreement between the observations and the predictions of the model is not just coincidence, but rather stems from the fact that we observed mainly radial variations rather than a mixture of radial and azimuthal variations.

8. Discussion

The above results provide a graphic and compelling demonstration of how the magnetic field and plasma patterns can change as solar wind flows interact between 1 AU and a few AU. On the one hand, shock formation in a simple, isolated corotating stream does appear to take place just as qualitative and quantitative theory would suggest. On the other hand, in the more common scenario of a solar wind with neighboring, interacting corotating and transient flows, it is seen that structures in the more distant solar wind, say at 4 or 5 AU, will be in fact a complex amalgam of dynamically merged flows, even though at that distance they may bear at least superficial resemblance to text-book CIR's resulting from large, isolated streams at 1 AU.

The dynamical process by which adjacent flows of varying spatial and temporal scales merge together at larger heliocentric distances has been described in the context of filtering (Gosling et al., 1976; see also the review by Holzer, 1979). That is, one of the most fundamental dynamical properties of the solar wind is the tendency for small scale flow structures to evolve more rapidly than large scale structures, such that at greater heliocentric distances only the largest scale structures remain, the smaller ones having been washed out (through dynamical exchange of momentum and energy with their surroundings) and subsequently swept up by the surviving larger ones. It is in this sense, then, that the solar wind is said to act as a low-pass filter. A fairly straightforward manifestation of this process is evident in our stream #3, the classic isolated flow case. Referring back to Figures 4 and 5, we call attention to the high frequency (short wavelength) fluctuations discerned in the 1 AU IMP velocity profile. By 1.74 AU (Figure 5), both the calculation and the real data show a marked loss of detail, a distinct smoothing of the profile. The effect is particularly noticeable in the trailing portions of the stream. Gosling et al. (1976), remarking upon the same phenomenon in their 1 AU to 4 AU mapping of IMP-Pioneer streams, ascribed the disappearance of the fluctuations in speed to rapid (relative to that of the overall waveform) steepening commensurate with their small scale, leading to shock formation andd degradation via dissipation. While shock formation and dissipation may have been a significant ingredient of the process within the context of the idealization of their model (an r-t hydrodynamic formulation known to overestimate the intensity of such interactions by virtue of its neglect of magnetic and nonradial flow effects), it is really only incidental to the dynamical evolution. That is, the essential process is that small scale structures evolve more rapidly and are eventually consumed by larger scale features. If the amplitudes of the small scale features are sufficiently large, shocks may form and indeed hasten the demise of the fluctuations; however that is not at all essential to the process, which can proceed to completion (albeit perhaps more slowly) by following a "subsonic" shock-free evolution (Hundhausen and Pizzo, unpublished manuscript; see also the discussion of "irregular fluctuations" in Burlaga, 1975). Finally, it should also be emphasized that it makes no fundamental difference whether the small scale structures are corotating or truly temporally varying; the evolution may proceed at different rates, but it will occur all the same, as demonstrated by streams 1 and 2 in this study.

For the smallest scale, smallest amplitude fluctuations, the dynamical evolution pretty much leads to oblivion, in the sense that all traces of their intrinsic velocity, thermodynamic, and magnetic structure are ultimately washed out beyond recognition by the larger scale, higher amplitude flows in which they become embedded. For the larger fluctuations, however, it is to be expected that their intrinsic structure might have an important impact upon the process and that some residue of the original variations might even be discernible at laarger heliocentric distances. This aspect of the evolutionary dynamics was also addressed in Gosling et al. (1976). In their examples, the individual velocity variations associated with several small scale streams lying at the leading edge of a much larger stream were observed to be smoothed out and virtually obliterated by 4 AU; but their associated compression fronts (which were quite distinct at 1 AU) had been merged together into a dynamical evolution. The mechanism for this merging, of course, is simply the kinematic advection of the larger scale, higher amplitude streams into the smaller ones together with the interaction of the individual pressure waves. Unfortunately, the Gosling et al. (1976) study was somewhat handicapped, in the sense that the start (1 AU) and end (4 AU) points of the process were all that could be observed (and then only the velocity profiles were available at 4 AU); the authors had to rely upon intuition and a numerical model to reconstruct what had happened in the intervening distances. The contribution of our study to this matter is that the IMP and Voyager data utilized herein, which are rather complete, captures the process in action and it shows that even quantitative details of the evolutionary process can be tracked with the appropriate model.

Recently, the importance of the cummulative effects of the dynamical interactions among various corotating and transient flows in the inner solar system upon the properties of the distant solar wind has received special emphasis (Burlaga, 1983). Indeed, the specific sweeping and merging (or coalescence) aspects of stream evolution have been accorded the specific designation "entrainment" (Burlage et al., 1983a). The entrainment of compression regions (such as occurs in our streams #1 and #2) has been shown to imply the transfer of magnetic energy from smaller to larger scales (Burlaga and Goldstein, 1983). It has been suggested that the magnetic field

structure of various kinds of flow systems (e.g., those consisting of predominantly corotating structures versus predominantly transient structures) at large heliocentric distances might differ somewhat with significant impact upon cosmic ray transport (Goldstein et al., 1984; Burlaga et al., 1983b).

Finally, the dynamical filtering of small scale, stream structures may also be taking place well inside 1 AU, though perhaps with some modifications. This is, near the sun, stationary corotating fluctuations could be expected to evolve only slowly, as the rotational mechanism driving the dynamics produces a very oblique interaction between adjacent stream tubes. Non-stationary fluctuations close to the sun, on the other hand, would in general possess more nearly radial gradients, and we might anticipate that they would be subject to stronger interactions. It is interesting to speculate that this tendency for the temporal fluctuations to be more strongly filtered near the sun which might have some bearing upon the afore-mentioned difficulties encountered by the models in treating the near sun evolution of cororating streams (see also Pizzo, 1983, 1984). This is, considerable low-amplitude fluctuations associated with the ever-present global coronal evolution should be present in the solar wind in the inner solar system. (Here we expressly exclude consideration of impulsive, large scale, transient systems, such as associated with flares.) Hence the evolution cannot strictly follow that expected for a single, absolutely corotating stream. Near and beyond 1 AU however, nearly all these short-period temporal variations would have been washed out, with only the largest amplitude, longest wavelength structures remaining. In this view, then, the relative success of corotating stream models at larger heliocentric distances cannot be attributed to the geometric diminution of nonradial flow effects alone. Rather, flow interactions and filtering may play a significant role, in that they act in such a way as to assure that the greater the heliocentric distance, the closer the remnant flow systems come to the steady idealization presumed in the models.

ACKNOWLEDGMENTS

We wish to thank the Principal Investigators of the Voyager plasma and magnetic field experiments, H. Bridge and N. F. Ness, respectively, for the data used in this paper. We also thank T. E. Holzer and A. J. Lazarus for reviewing the manuscript and offering helpful comments. The National Center for Atmospheric Research is sponsored by the National Science Foundation.

REFERENCES

Burlaga, L. F., A reverse hydromagnetic shock in the solar wind, Cosmic Electrodynamics, 1 233, 1970.

Burlaga, L. F., Interplanetary streams and their interaction with the earth, Space Sci. Rev., 17, 327, 1975.

Burlaga, L. F., Corotating pressure waves without fast streams in the solar wind, J. Geophys. Res., 88, 6085, 1983.

Burlaga, L. F., and E. Barouch, Interplanetary stream magnetism: Kinematic effects, Astrophys. J., 203, 257, 1976.

Burlaga, L. F. and M. L. Goldstein, Radial variations of large-scale magnetohydrodynamic fluctuations in the solar wind, NASA TM 85116, 1983, submitted to J. Geophys. Res.

Burlaga, L. F. and K. W. Ogilvie, Magnetic and thermal pressures in the solar wind, Solar Phys., 15, 61, 1970.

Burlaga, L. F., R. Lepping, R. Weber, T. Armstrong, C. Goodrich, J. Sullvian, D. Gurnett, P. Kellogg, E. Keppler, F. Mariani, F. Neubauer, H. Rosenbauer, and R. Schwenn, Interplanetary particles and fields, Nov. 22 to Dec. 6, 1977: Helios, Voyager observations between 0.6 and 1.6 AU, J. Geophys. Res., 85, 2227, 1980.

Burlaga, L. F., N. F. Ness, F. Mariani, B. Bavassano, U. Villante, H. Rosenbauer, R. Schwenn, and J. Harvey, Magnetic fields and flows between 1 and 0.3 AU during the primary mission of Helios 1, J. Geophys. Res., 83, 5167, 1978.

Burlaga, L., R. Schwenn and H. Rosenbauer, Dynamical evolution of interplanetary magnetic fields and flows between 0.3 AU and 8.5 AU; Entrainment, Geophys. Res. Lett., 10, 413, 1983a.

Burlaga, L. F., F. B. McDonald, N. F. Ness, R. Schwenn, A. J. Lazarus, F. Mariani, Interplanetary flow systems associated with cosmic ray modulation in 1977-1980, NASA TM 85120, 1983b.

Collard, H. P., J. D. Mihalov, and J. H. Wolfe, Radial variation of the solar wind speed between 1 and 15 AU, J. Geophys., 87, 2203, 1982.

Dryer, M., and R. S. Steinolfson, MHD solution of interplanetary disturbances generated by simulated velocity perturbations, J. Geophys. Res., 81, 5413, 1976.

Dryer, M., Z. K. Smith, E. J. Smith, J. D. Mihalev, J. H. Wolfe, R. S. Steinolfson, and S. T. Wu, Dynamic MHD modeling of solar wind corotating stream interaction regions observed by Pioneer 10 and 11, J. Geophys. Res., 83, 4347, 1978.

Goldstein, B. E., Nonlinear corotating solar wind strucutre, Rep. CSR-P-71-63, Mass. Inst. of Technol., Cambridge, 1971.Goldstein, B. E., Nonlinear corotating solar wind strucutre, Rep. CSR-P-71-63, Mass. Inst. of Technol., Cambridge, 1971.

Goldstein, B. E., and J. R. Jokipii, Effects of stream-associated fluctuations upon the radial evolution of average solar wind parameters, J. Geophys. Res., 82, 1095, 1977.

Goldstein, M. L., L. F. Burlaga, and W. H. Matthaeus, Power spectral signatures of interplanetary corotating and transient flows, NASA TM 86051, submitted to J. Geophys. Res., (in press) 1984.

Gosling, J. T., Solar wind stream evolution, Solar Wind Four, edited by H. Rosenbauer, Report No. MPAE-W-100-81-31, p. 107, 1981.

Gosling, J. T., A. J. Hundhausen, and S. J. Bame, Solar wind evolution at large heliocentric distances: Experimental demonstration and the test of a model, J. Geophys. Res., 81, 2111, 1976.

Holzer, T. E., The solar wind and related astrophysical phenomena, in Solar System Plasma Physics, Vol. 1, E. N. Parker, C. F. Kennel, and L. J. Lanzerott, eds., North-Holland, 1979.

Hundhausen, A. J., Coronal Expansion and Solar Wind, Springer-Verlag, New York, 1972.

Hundhausen, A. J., A Non-linear model of high-speed solar wind streams, J. Geophys. Res., 78, 1528, 1973a.

Hundhausen, A. J., Evolution of large-scale solar wind structures beyond 1 AU, J. Geophys. Res., 78, 2035, 1973b.

Hundhausen, A. J. and J. T. Gosling, Solar wind structure at large heliocentric distances, An interpretation of Pioneer 10 observations, J. Geophys. Res., 81, 1436, 1976.

King, J. H., Interplanetary Medium Data Book, Supplement 1, NSSPC/WPC-A-RAS, 79-04, 1979.

MacCormack, R. W., Numerical solution of the interaction of a shock wave with a laminar boundary layer, in Proceedings of the Second International Conference on Numerical Methods in Fluid Dynamics Lecture Notes in Physics, Vol. 8, edited by M. Holt, p. 151, Springer, New York, 1971.

Parker, E. N., Interplanetary Dynamical Processes, Interscience Publishers, New York, 1963.

Pizzo, V., A three-dimensional model of corotating streams in the solar wind, Hydrodynamic streams, J. Geophys. Res., 85, 727, 1980.

Pizzo, V., An evaluation of corotating solar wind stream models, in Solar Wind Four, H. Rosenbauer, ed., MPAE-W-100-81-31, Liindau, FRG, p. 153, 1981.

Pizzo, V. J., A three-dimensional model of corotating streams in the solar wind. Magnetodyrodynamic streams, J. Geophys. Res., 87, 4374, 1982.

Pizzo, V., Quasi-Steady Solar Wind Dynamics, Solar Wind Five, in press, 1983.

Pizzo, V., Interplanetary shocks on the large scale--A retrospective on the last decade's theoretical efforts, in the Proceedings of the Napa Valley Chapman Conference on Collisionless Shocks, R. Stone, ed., to be published, 1984.

Rhodes, E. J., Jr., and E. J. Smith, Multi-spacecraft observations of heliographic latitude-longitude structure in the solar wind, J. Geophys. Res., 86, 8877, 1981.

Sarabhai, V., Some consequences of nonuniformity of solar wind velocity, J. Geophys. Res., 68, 1555, 1963.

Scudder, J. D. and S. Olbert, A theory of local and global processes which affect solar wind electrons 1. The origin of typical 1 AU velocity distribution functions, J. Geophys. Res., 84, 2755, 1979a.

Scudder, J. D. and S. Olbert, A theory of local and global processes which affect solar wind electrons. 2. Experimental support, J. Geophys. Res., 84, 6603, 1979b.

Sittler, E. C. Jr., and J. D. Scudder, An empirical polytrope law for solar wind thermal electrons between 0.45 and 4.76 AU: Voyager 2 and Mariner 10, J. Geophys. Res., 85, 5131, 1980.

Smith, E. J., and J. H. Wolfe, Observations of interaction regions and corotating shocks between one and five AU: Pioneers 10 and 11, Geophys. Res. Lett., 3, 137, 1976.

Whang, Y. C., and T. H. Chien, Magnetohydrodynamic interaction of high speed streams, J. Geophys. Res., 86, 3263, 1981.

FIGURE CAPTIONS

Figure 1 (Top) Speed profile measured by Imps 7 and 8 showing the three flows discussed in the paper; the polarity of the interplanetary magnetic field is also shown. (Bottom) K-coronameter polarization brightness contours, showing the location of coronal holes.

Figure 2 Trajectories of Imps 7, 8 and Voyagers 1, 2, in inertial heliographic coordinates. The angle λ is the heliographic latitude of the spacecraft.

Figure 3 Five minute averages of the magnetic field and plasma data for stream 3, showing a stream interface at the leading edge of a corotating stream.

Figure 4 (Left) Magnetic field strength, plasma parameters, and total pressure for stream 3 observed at 1 AU. (Right) The corresponding parameters calculated for 2 AU, showing a forward shock (FS) and a reverse shock (RS).

Figure 5 Magnetic field strength, plasma parameters and total pressure versus Carrington longitude. Predicted values from the MHD model with IMP data at 1 AU as input are shown by the solid curves. Observed values are shown by the dots.

Figure 6 High temporal resolution data of stream 3 from Voyager 1, confirming the existence of a forward-reverse shock pair at 1.74 AU.

Figure 7 Theoretical curves for the speed and field strength at 2, 3 and 4 AU, together with the profiles measured at 1 AU.

Figure 8 Five minute averages of the magnetic field and plasma data for stream 1, showing a forward shock (FS), two stream interfaces (IF), and a possible reverse shock (RS?).

Figure 9 (Left) Magnetic field strength, plasma parameters and the total pressure (magnetic plus thermal) for stream 1 observed at 1 AU. Two compression regions are indicated by the shaded areas in P_T, one for the slow stream and one for the fast stream. (Right) the corresponding parameters calculated for 2 AU. A single broad compression is visible at 2 AU, implying the coalescence of the two shown on the left.

Figure 10 Magnetic field strength, plasma parameters and total pressure versus Carrington longitude. Predicted values from the MHD model with IMP data at 1 AU as input are shown by the solid curves. Observed values are shown by the dots.

Figure 11 Theoretical curves for the speed and field strength at 2, 3, and 4 AU, together with the profiles measured at 1 AU. Note the coalescence at the two peaks in B between 1 AU and 2 AU, the coalescence of the 2 forward shocks near 4 AU, and the coalescence of the 2 reverse shocks near 3 AU.

Figure 12 Five minute averages of the magnetic field and plasma data for stream 2, showing a forward shock (F1), an interface (IF), a possible site for formation of a reverse shock (RS), and a possible forward shock (FS).

Figure 13 (Left) Magnetic field strength, plasma parameters, and total pressure for stream 2 observed at 1 AU. (Right) The corresponding parameters computed for 2 AU. Two pressure waves observed at 1 AU coalesce to form a single pressure wave at 2 AU.

Figure 14 Magnetic field strength, plasma parameters and total pressure versus Carrington longitude. Predicted values from the MHD model with IMP data at 1 AU as input are shown by the solid curves. Observed values are shown by the dots.

Figure 15 Theoretical curves for the speed and field strength at 2 AU and 3 AU, together with the profiles measured at 1 AU. Note the coalescence of the shocks and of the pressure waves.

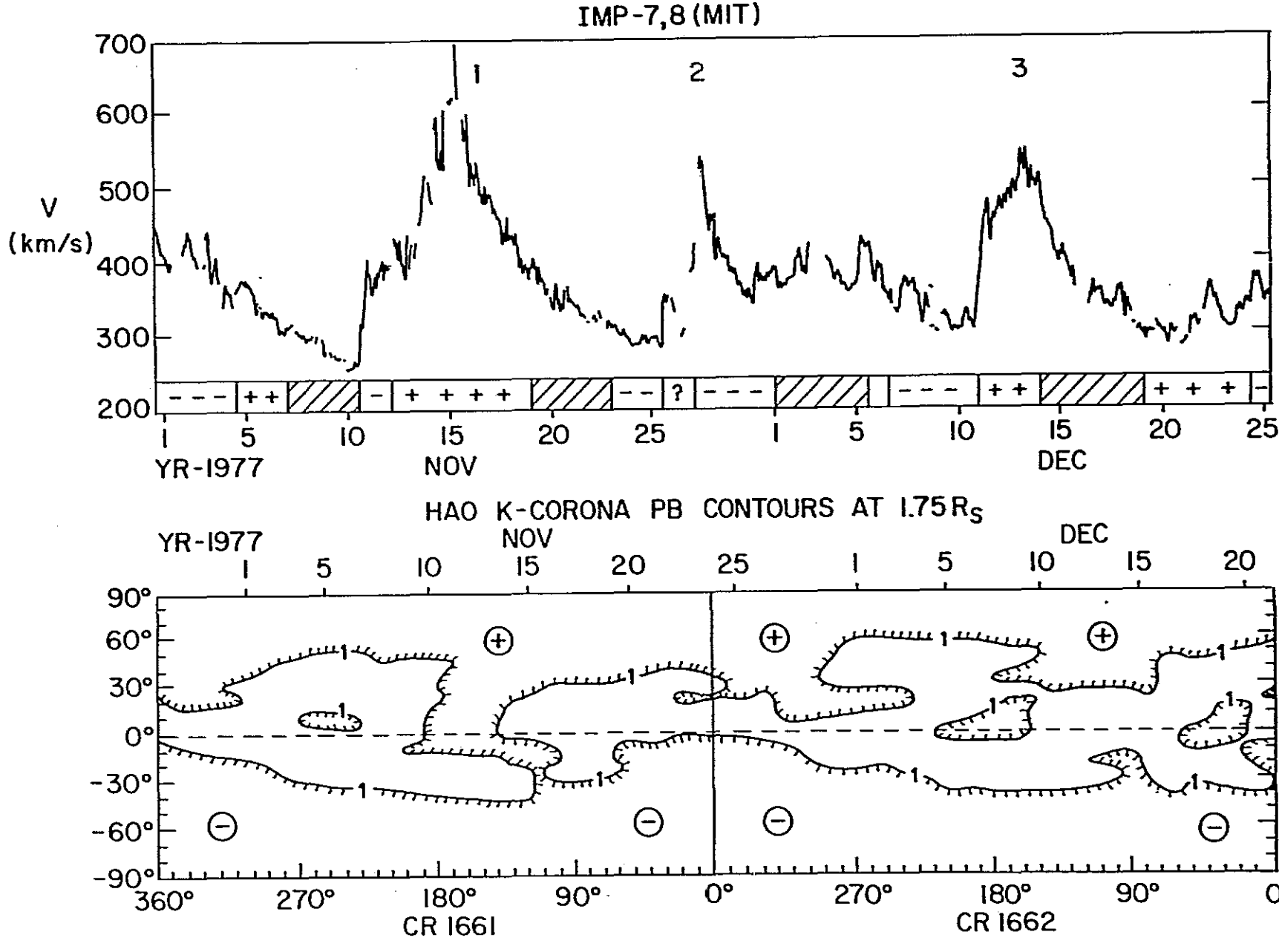
IMP-7,8 (MIT)
V
(km/s)
700
600
500
400
300
200
1
2
3
- - -
+ +
?
1
5
10
15
20
25
YR-1977
NOV
DEC
HAO K-CORONA PB CONTOURS AT 1.75 R_S
90°
60°
30°
0°
-30°
-60°
-90°
360°
270°
180°
90°
0°
CR 1661
CR 1662

Figure 1

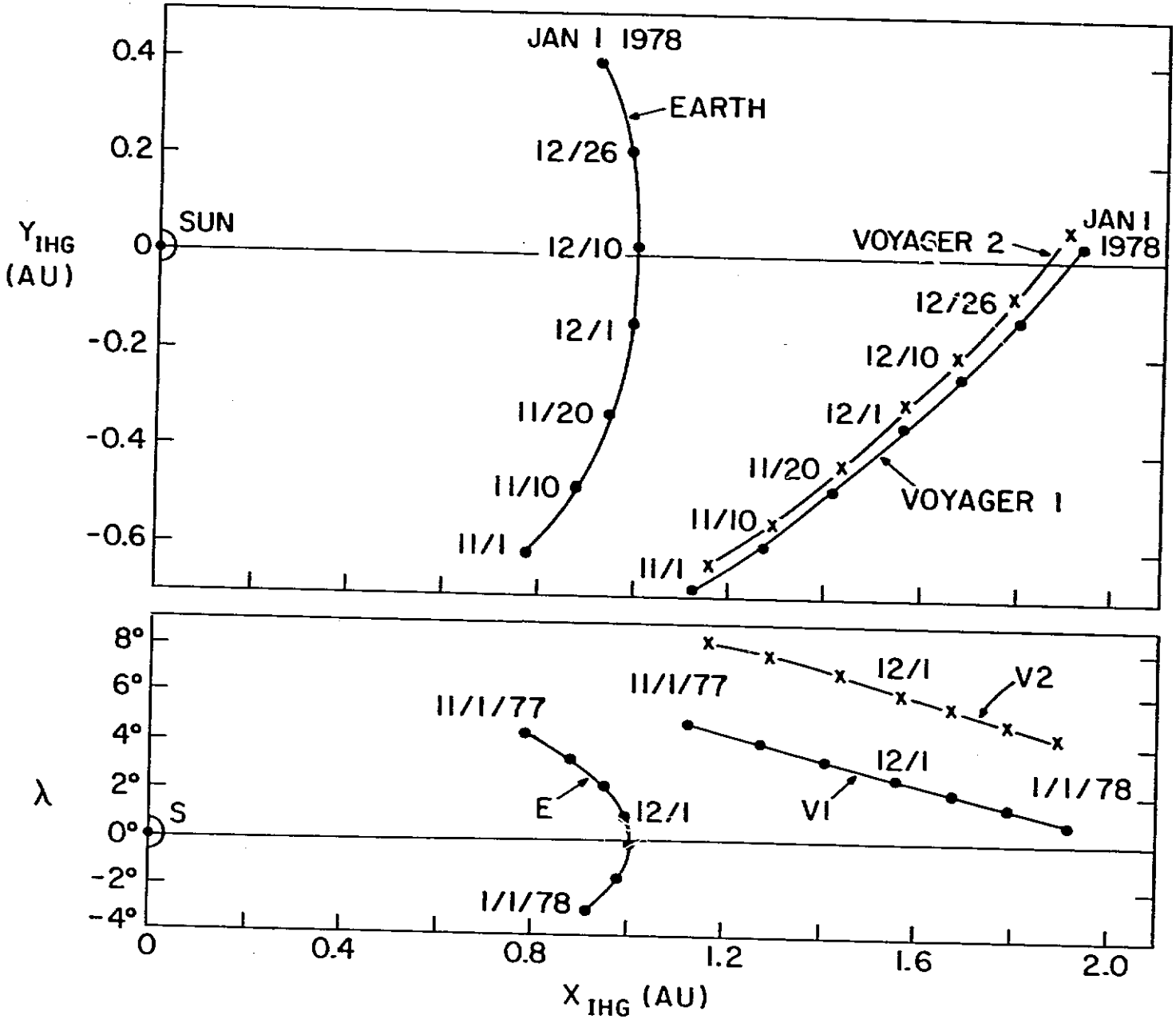
JAN 1 1978
EARTH
12/26
12/10
12/1
11/20
11/10
11/1
SUN
VOYAGER 2
JAN 1
1978
12/26
12/10
12/1
11/20
11/10
11/1
VOYAGER 1
0.4
0.2
0
-0.2
-0.4
-0.6
Y_{IHG} (AU)
11/1/77
12/1
V2
11/1/77
12/1
E
12/1
V1
1/1/78
S
1/1/78
8°
6°
4°
2°
0°
-2°
-4°
λ
0
0.4
0.8
1.2
1.6
2.0
X_{IHG} (AU)

Figure 2

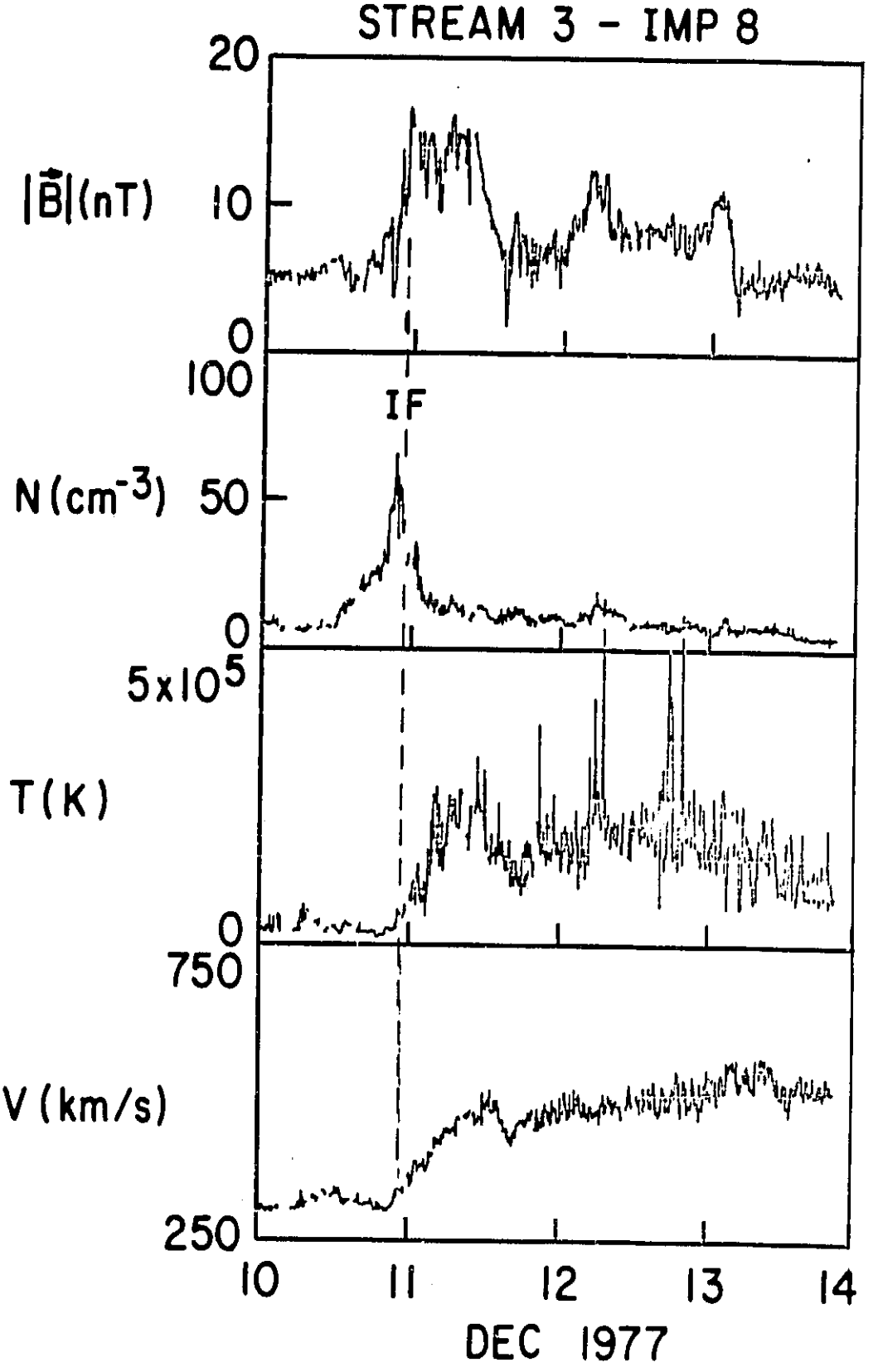
STREAM 3 - IMP 8
20
10
0
|B|(nT)
100
50
0
IF
N(cm-3)
5x10^5
0
T(K)
750
250
V (km/s)
10
11
12
13
14
DEC 1977

Figure 3

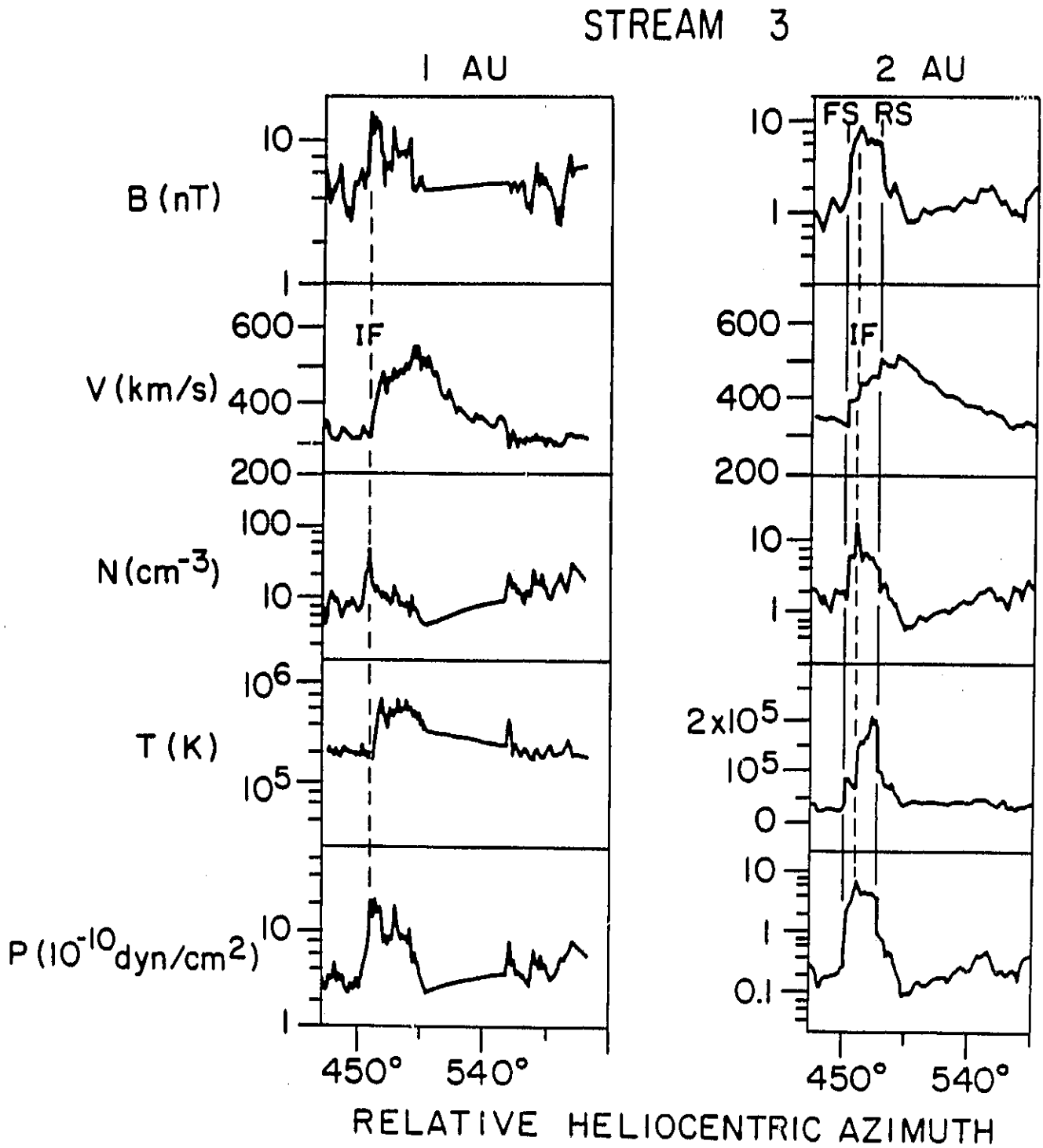
STREAM 3
1 AU
2 AU
B (nT)
V (km/s)
N (cm⁻³)
T (K)
P (10⁻¹⁰ dyn/cm²)
IF
FS
RS
450°
540°
RELATIVE HELIOCENTRIC AZIMUTH

Figure 4

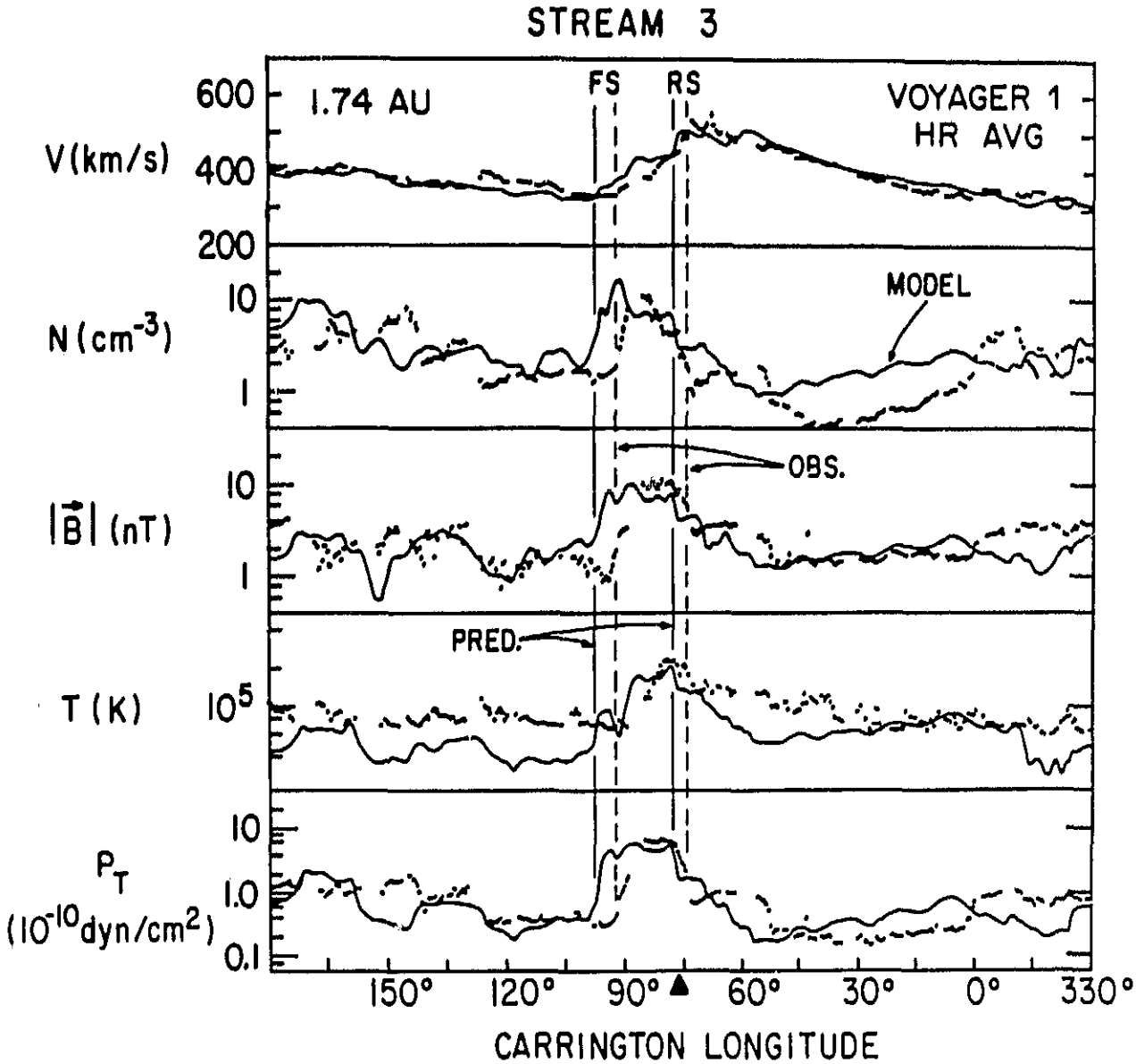
STREAM 3
1.74 AU
FS
RS
VOYAGER 1
HR AVG
V(km/s)
600
400
200
N(cm⁻³)
10
1
MODEL
|B| (nT)
OBS.
PRED.
T(K)
10⁵
P_T
(10⁻¹⁰dyn/cm²)
1.0
0.1
150°
120°
90°
60°
30°
0°
330°
CARRINGTON LONGITUDE

Figure 5

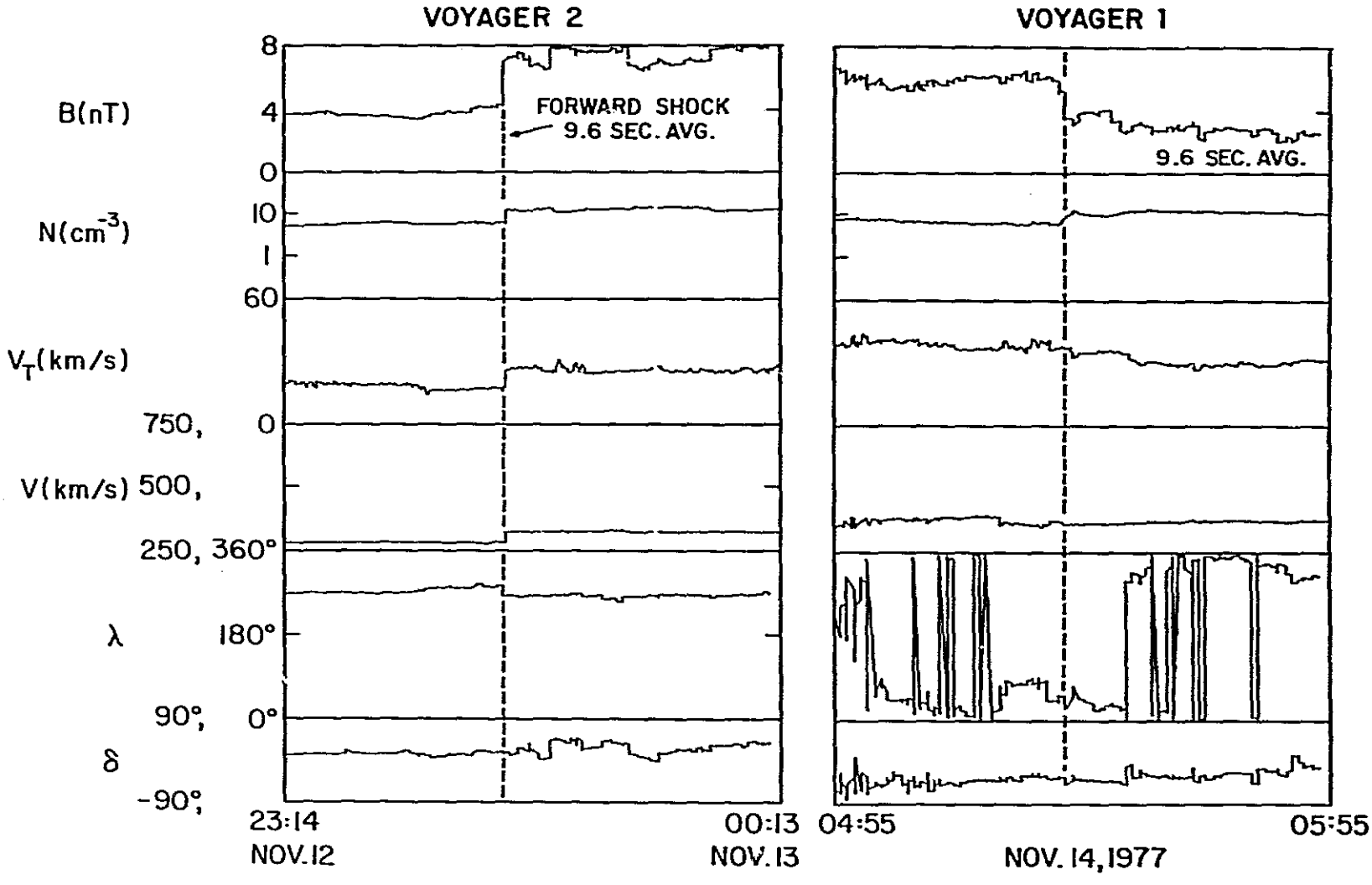
VOYAGER 2
VOYAGER 1
B(nT)
8
4
0
FORWARD SHOCK
9.6 SEC. AVG.
9.6 SEC. AVG.
N(cm⁻³)
10
1
VT(km/s)
60
750,
0
V(km/s)
500,
250,
360°
λ
180°
90°,
0°
δ
-90°,
23:14
NOV.12
00:13
NOV.13
04:55
05:55
NOV. 14,1977

Figure 6

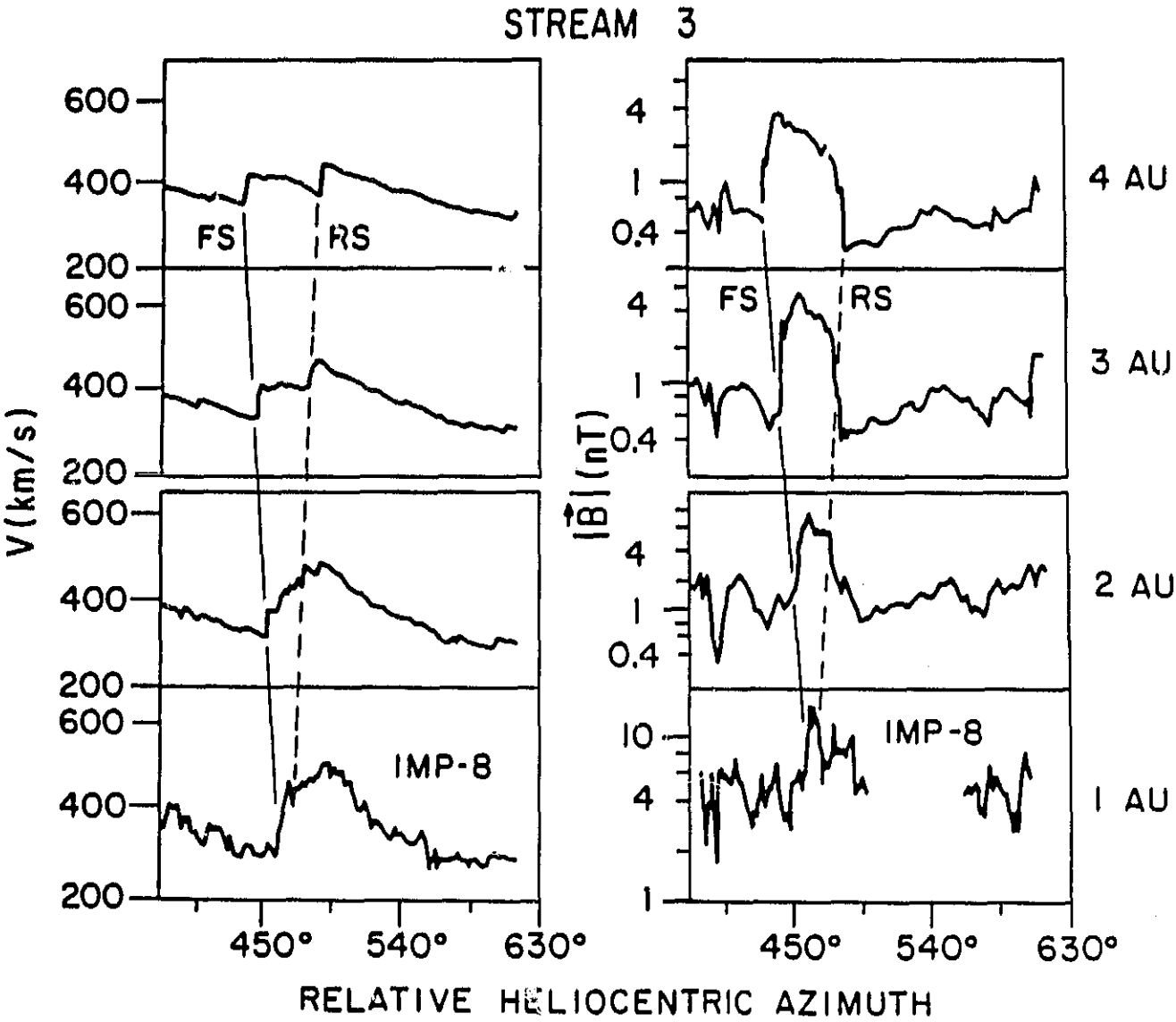
STREAM 3
V(km/s)
600
400
200
FS
RS
IMP-8
|B| (nT)
4
1
0.4
10
4
1
4 AU
3 AU
2 AU
1 AU
450°
540°
630°
RELATIVE HELIOCENTRIC AZIMUTH

Figure 7

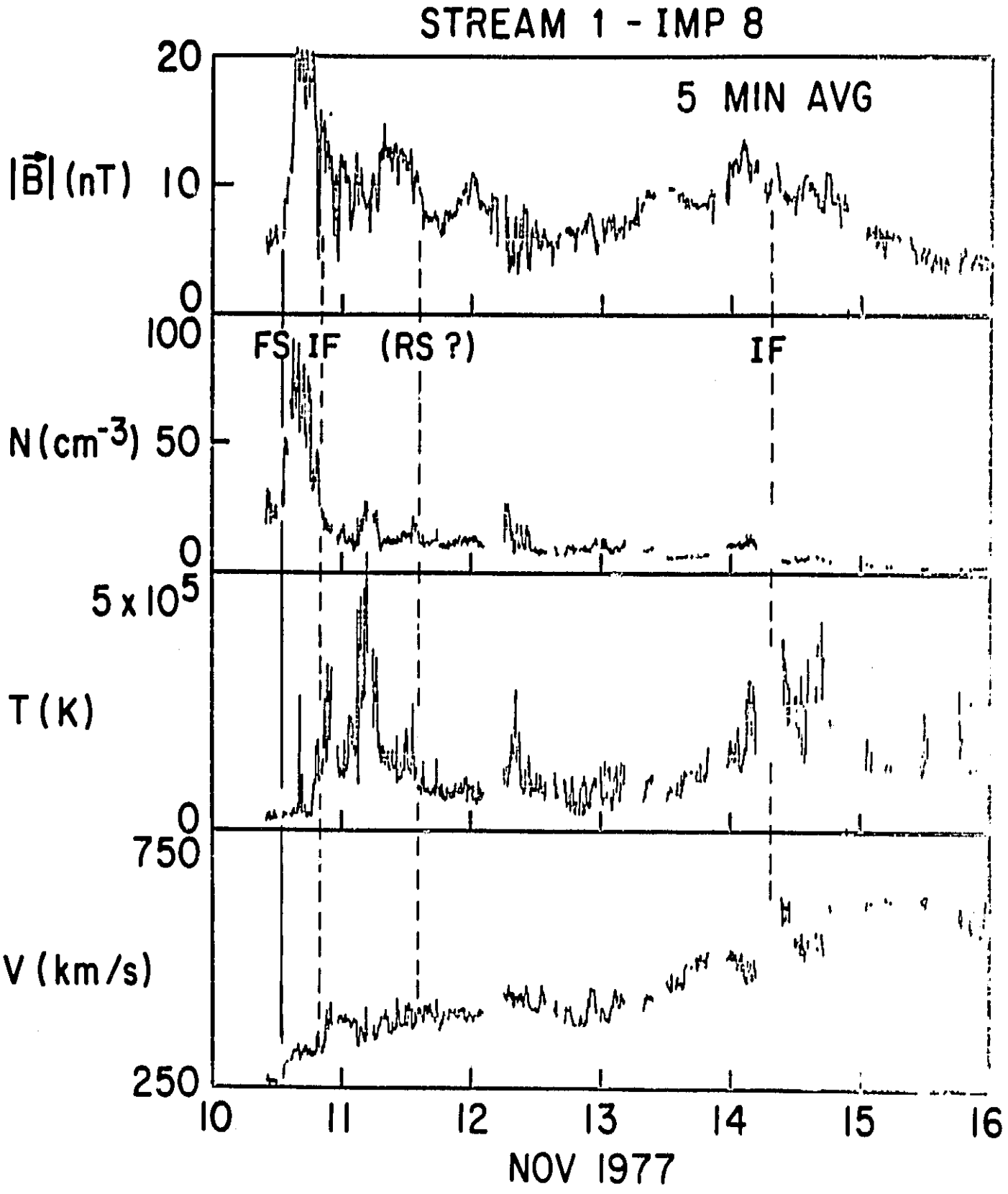
STREAM 1 - IMP 8
5 MIN AVG
|B| (nT)
20
10
0
FS
IF
(RS ?)
IF
N (cm-3)
100
50
0
5 x 10^5
T (K)
0
750
V (km/s)
250
10
11
12
13
14
15
16
NOV 1977

Figure 8

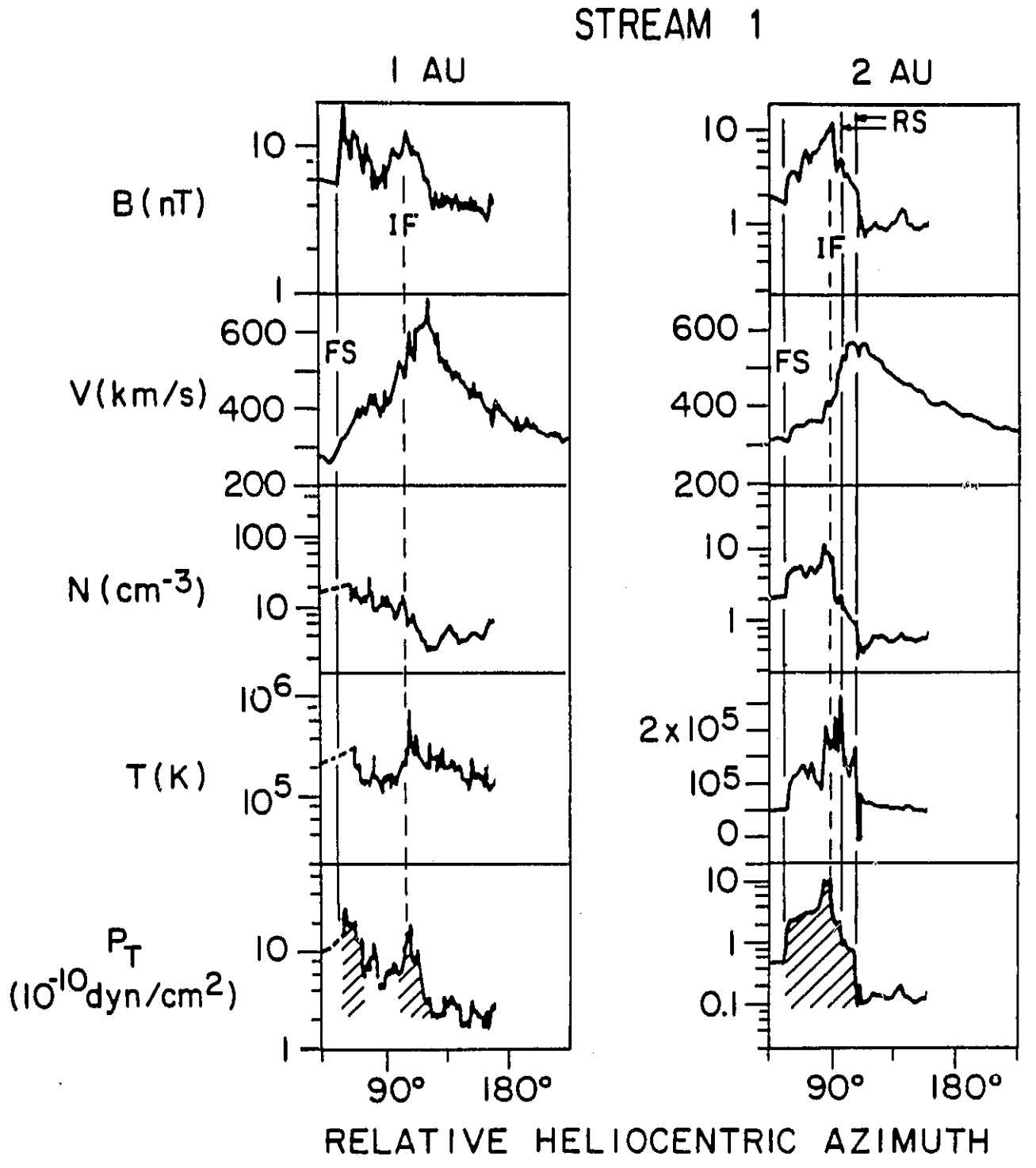
STREAM 1
1 AU
2 AU
B (nT)
V (km/s)
N (cm⁻³)
T (K)
P_T
(10⁻¹⁰ dyn/cm²)
IF
FS
RS
10
1
600
400
200
100
10⁶
10⁵
2x10⁵
0
0.1
90°
180°
RELATIVE HELIOCENTRIC AZIMUTH

Figure 9

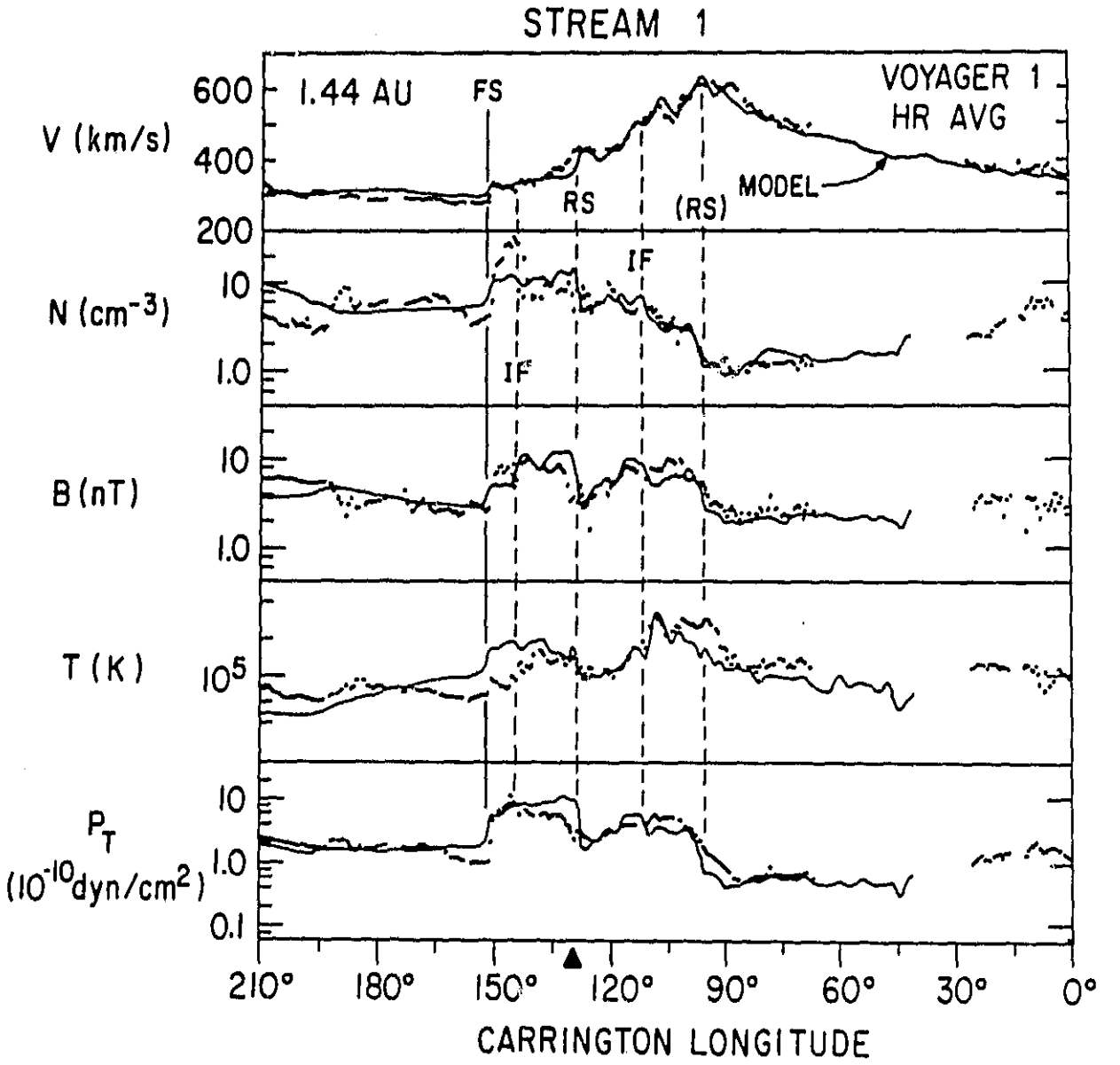
STREAM 1
1.44 AU
FS
VOYAGER 1
HR AVG
V (km/s)
600
400
200
RS
(RS)
MODEL
IF
N (cm⁻³)
10
1.0
IF
B (nT)
10
1.0
T (K)
10⁵
P_T
(10⁻¹⁰dyn/cm²)
10
1.0
0.1
210°
180°
150°
120°
90°
60°
30°
0°
CARRINGTON LONGITUDE

Figure 10

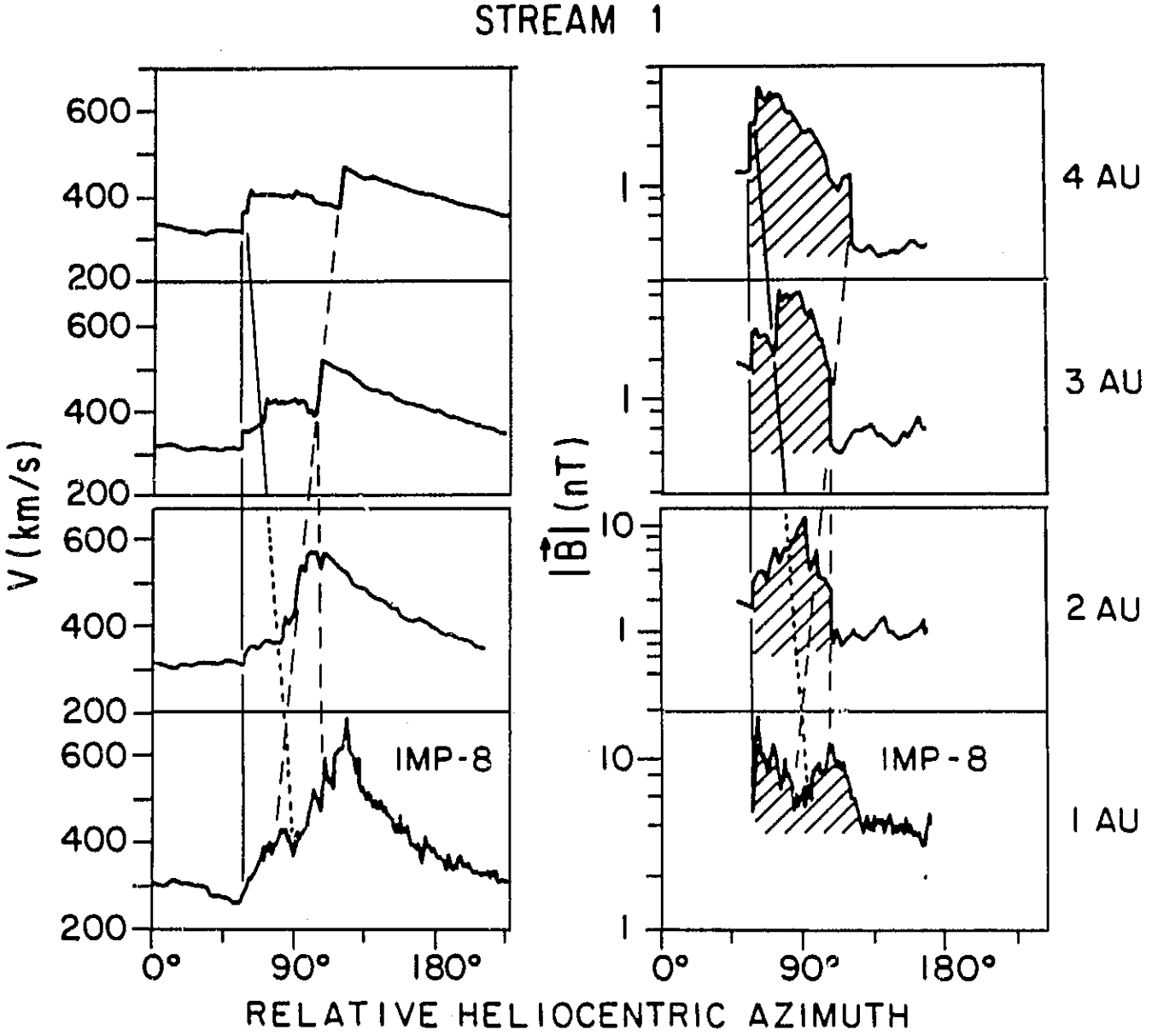
STREAM 1
V (km/s)
600
400
200
|B| (nT)
10
1
4 AU
3 AU
2 AU
1 AU
IMP-8
0°
90°
180°
RELATIVE HELIOCENTRIC AZIMUTH

Figure 11

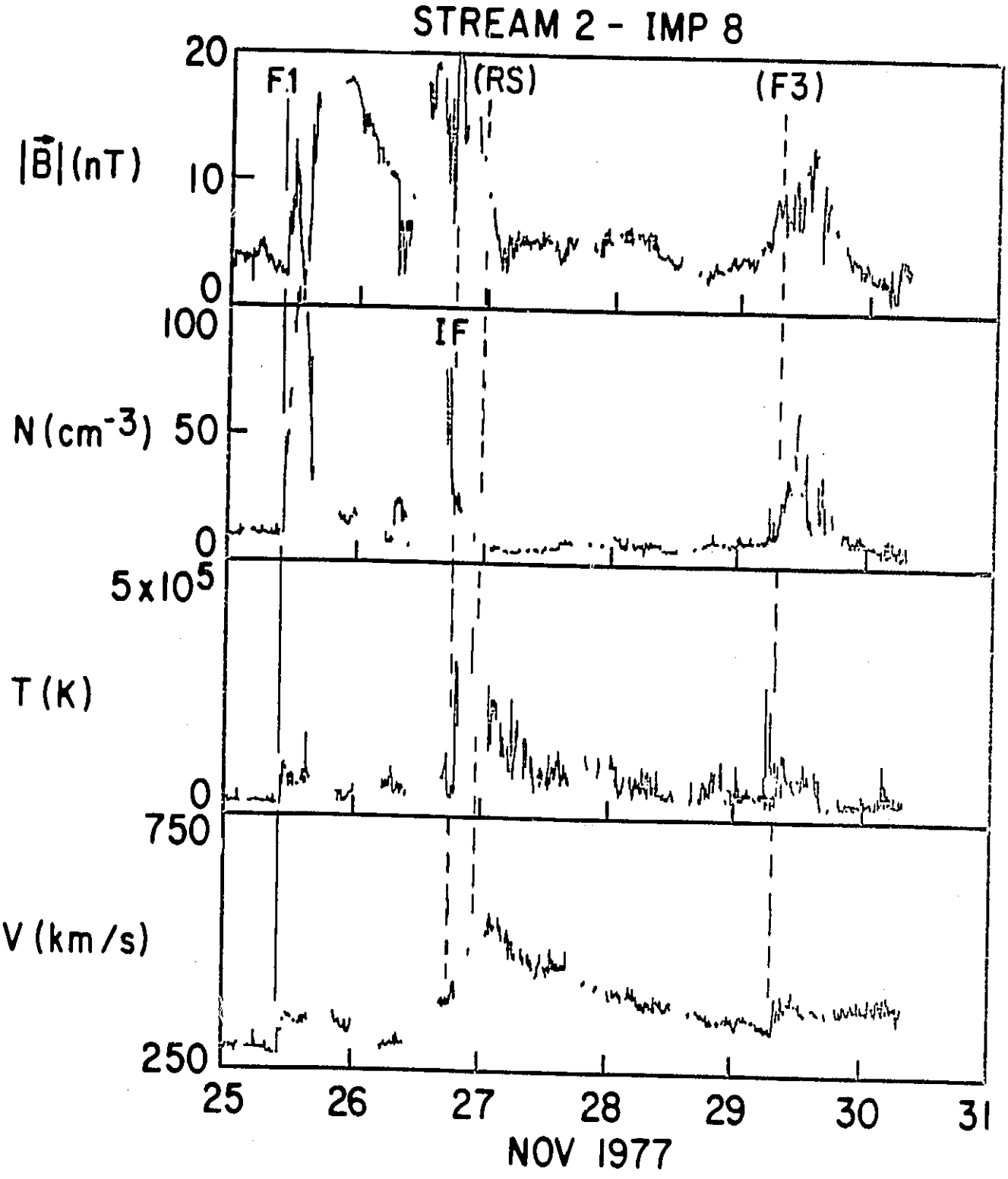
STREAM 2 - IMP 8
20
10
0
F1
(RS)
(F3)
|B| (nT)
100
50
0
IF
N (cm-3)
5x10^5
0
T (K)
750
250
V (km/s)
25
26
27
28
29
30
31
NOV 1977

Figure 12

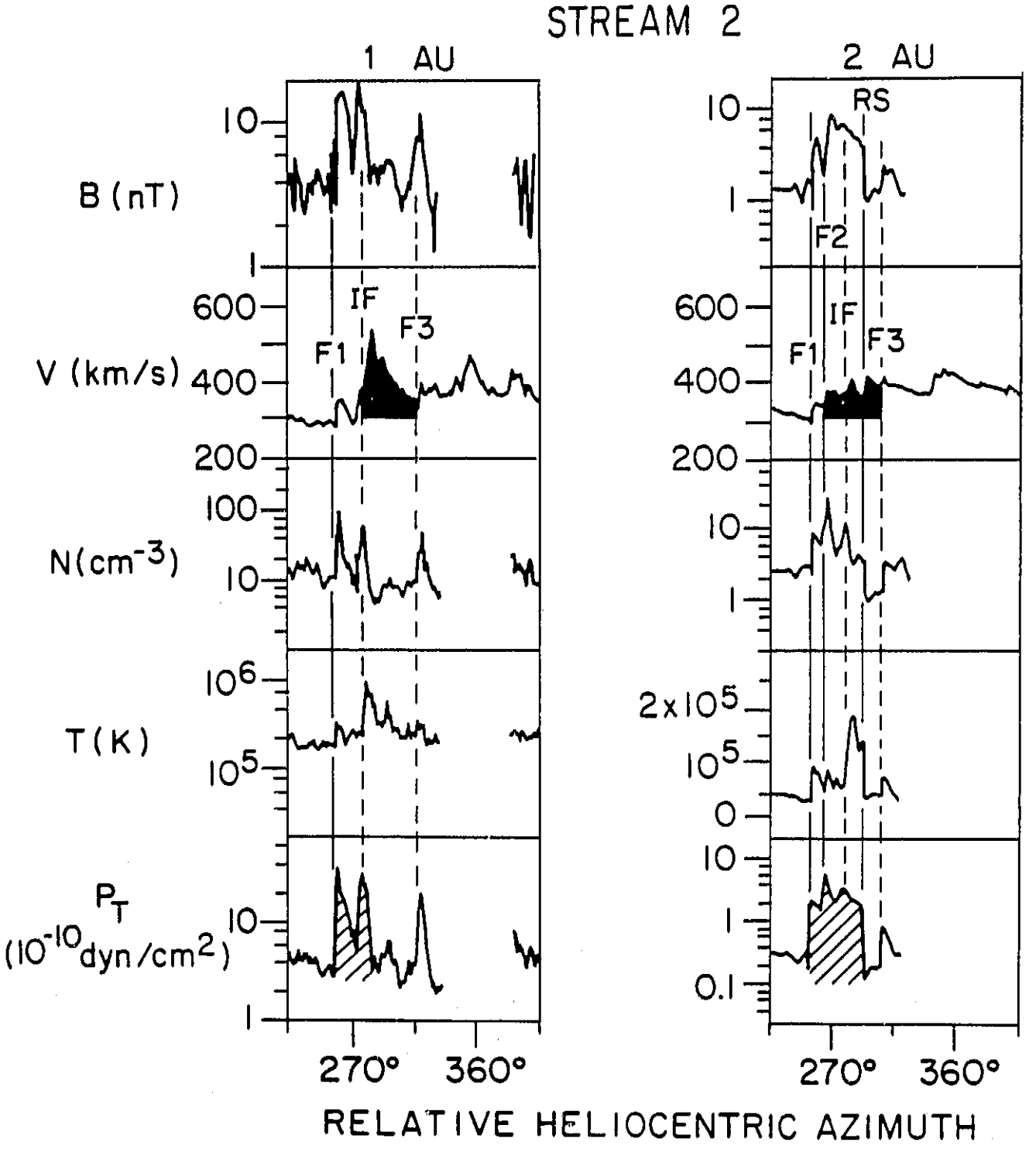
STREAM 2
1 AU
2 AU
B (nT)
V (km/s)
N(cm⁻³)
T(K)
P_T
(10⁻¹⁰dyn/cm²)
IF
F1
F2
F3
RS
270°
360°
RELATIVE HELIOCENTRIC AZIMUTH

Figure 13

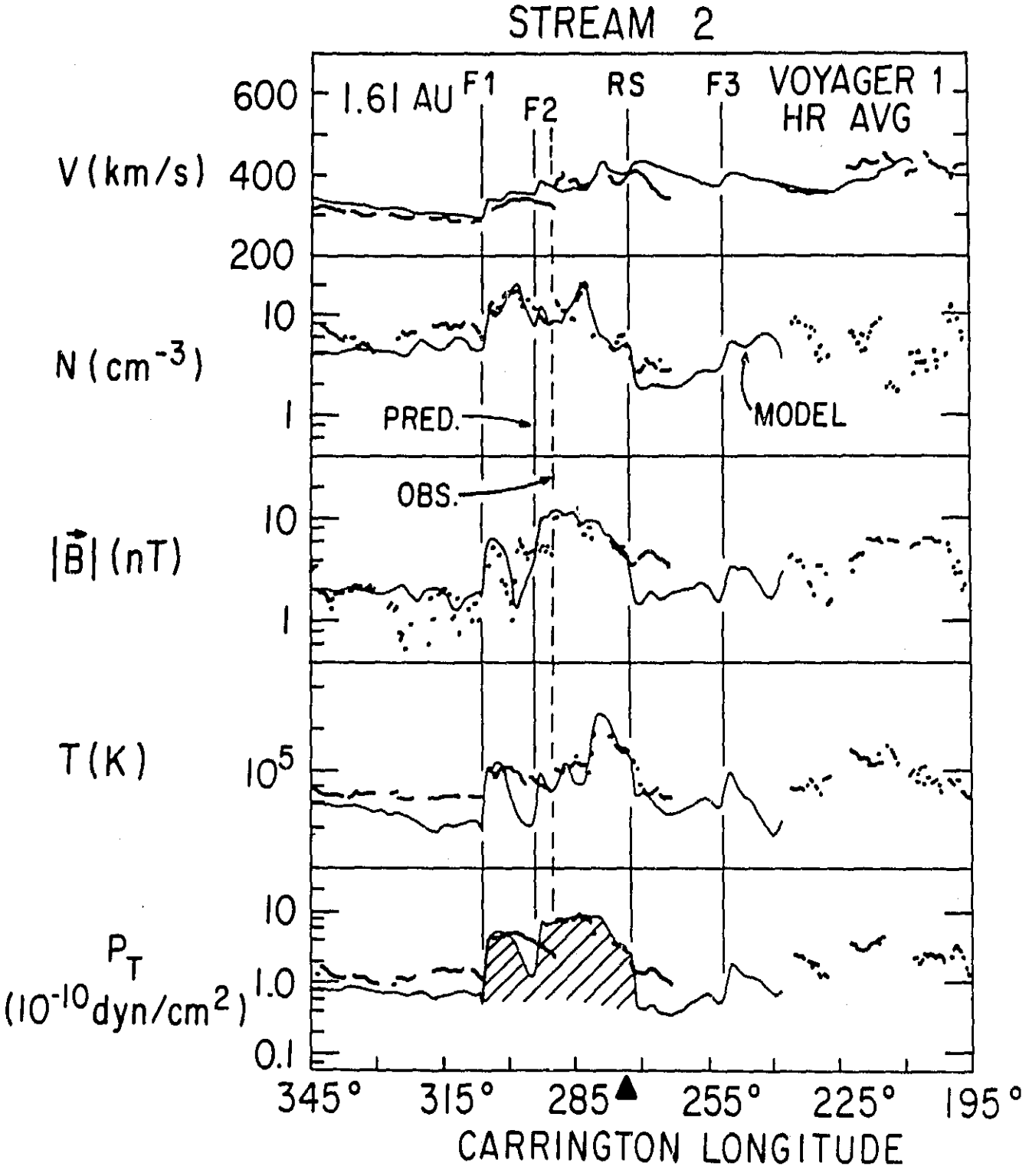
STREAM 2
1.61 AU
F1
F2
RS
F3
VOYAGER 1
HR AVG
V (km/s)
600
400
200
N (cm⁻³)
10
1
PRED.
MODEL
OBS.
|B| (nT)
10
1
T (K)
10⁵
P_T
(10⁻¹⁰ dyn/cm²)
10
1.0
0.1
345°
315°
285°
255°
225°
195°
CARRINGTON LONGITUDE

Figure 14

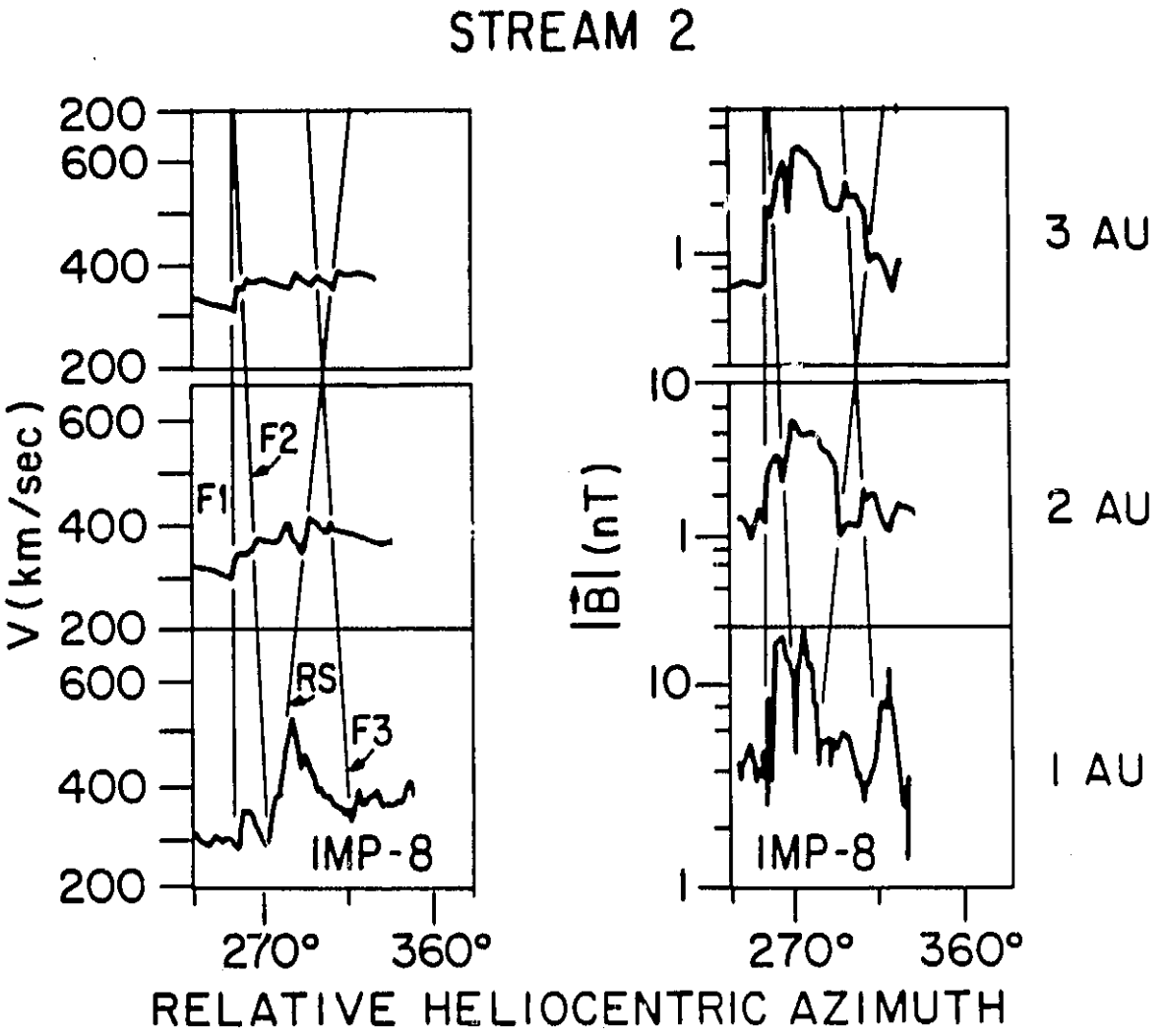
STREAM 2
200
600
400
200
600
400
200
600
400
200
V (km/sec)
F1
F2
RS
F3
IMP-8
270°
360°
|B| (nT)
10
1
10
1
1
IMP-8
270°
360°
3 AU
2 AU
1 AU
RELATIVE HELIOCENTRIC AZIMUTH

Figure 15

BIBLIOGRAPHIC DATA SHEET

1. Report No.	2. Government Accession No.	3. Recipient's Catalog No.
TM 86086		

4. Title and Subtitle	5. Report Date
Stream Dynamics between 1 AU and 2 AU: A Detailed Comparison of Observations and Theory	April 1984
	6. Performing Organization Code
7. Author(s) L. Burlaga, V. Pizzo, A. Lazarus and P. Gazis	8. Performing Organization Report No.
9. Performing Organization Name and Address NASA/GSFC Laboratory for Extraterrestrial Physics Interplanetary Physics Branch, Code 692 Greenbelt, MD 20771	10. Work Unit No.
	11. Contract or Grant No.
	13. Type of Report and Period Covered Technical Memorandum
12. Sponsoring Agency Name and Address	14. Sponsoring Agency Code

15. Supplementary Notes

16. Abstract

SEE ATTACHED.

17. Key Words (Selected by Author(s))	18. Distribution Statement
Solar wind, interplanetary magnetic field, shocks, streams	

19. Security Classif. (of this report)	20. Security Classif. (of this page)	21. No. of Pages	22. Price*
U	U	48	

*For sale by the National Technical Information Service, Springfield, Virginia

GSFC 25-44 (10/77)